

# 1 **High-resolution Kilometre-scale simulations over Fennoscandia** 2 **reveal a large loss of ~~Fennoscandian~~ tundra due to climate** 3 **warming change**

4 Fredrik Lagergren<sup>1</sup>, Robert G. Björk<sup>2, 3</sup>, Camilla ~~Andersson~~<sup>5</sup>Andersson<sup>4</sup>, Danijel ~~Belušić~~<sup>5</sup>Be-  
5 lušić<sup>4, 5, 6</sup>, Mats P. Björkman<sup>2, 3</sup> ~~now at 6~~, Erik ~~Kjellström~~<sup>5</sup>Kjellström<sup>4</sup>, Petter Lind<sup>4, 5</sup>, David Lind-  
6 stedt<sup>4, 5</sup>, Tinja Olenius<sup>4, 5</sup>, Håkan Pleijel<sup>6, 4</sup>, Gunhild Rosqvist<sup>7</sup> and Paul A. Miller<sup>1</sup>

7 <sup>1</sup>Department of Physical Geography and Ecosystem Science, Lund University, Lund, 223 62, Sweden

8 <sup>2</sup>Department of Earth Sciences, University of Gothenburg, Gothenburg, 405 30, Sweden

9 <sup>3</sup>Gothenburg Global Biodiversity Centre, Gothenburg, 405 30, Sweden

10 ~~<sup>4</sup>Swedish Meteorological and Hydrological Institute, Norrköping, 601 76, Sweden~~

11 <sup>5</sup>Department of Geophysics, Faculty of Science, University of Zagreb, Zagreb, 10 000, Croatia

12  
13 <sup>4, 6</sup>Department of Biological & Environmental Sciences, University of Gothenburg, Gothenburg, 405 30, Sweden

14 ~~<sup>5</sup>Swedish Meteorological and Hydrological Institute, Norrköping, 601 76, Sweden~~

15 ~~<sup>6</sup>Department of Geophysics, Faculty of Science, University of Zagreb, Zagreb, 10 000, Croatia~~

16 <sup>7</sup>Department of Physical Geography, Stockholm University, Stockholm, 106 91, Sweden

17  
18 *Correspondence to:* Fredrik Lagergren (Fredrik.Lagergren@nateko.lu.se)

19 **Abstract.** The Fennoscandian boreal and mountain regions harbour a wide range of vegetation types, from boreal  
20 forest to high alpine tundra and barren soils. The area is facing a rise in air temperature above the global average  
21 and changes in temperature and precipitation patterns. This is expected to alter the Fennoscandian vegetation  
22 composition and change the conditions for areal land-use such as forestry, tourism and reindeer husbandry. In this  
23 study we used a unique high-resolution (3 km) climate scenario with considerable warming resulting from strongly  
24 increasing carbon dioxide emissions to investigate how climate change can alter the vegetation composition, bio-  
25 diversity and availability of suitable reindeer forage. Using a dynamical vegetation model, including a new im-  
26 plementation of potential reindeer grazing, resulted in simulated vegetation maps of unprecedented high resolution  
27 for such a long time period and spatial extent. The results were evaluated at the local scale using vegetation  
28 inventories and for the whole area against satellite-based vegetation maps. A deeper analysis of vegetation shifts  
29 related to statistics of threatened species was performed in six “hotspot” areas containing records of rare and  
30 threatened species. **In this high emission scenario,** ~~T~~the simulations show dramatic shifts in the vegetation com-  
31 position, accelerating at the end of the century. Alarmingly, the results suggest the southern mountain alpine  
32 region in Sweden will be completely covered by forests at the end of the 21<sup>st</sup> century, making preservation of  
33 many rare and threatened species impossible. In the northern alpine regions, most vegetation types will persist but  
34 shift to higher elevations with reduced areal extent, endangering vulnerable species. Simulated potential for

35 reindeer grazing indicates latitudinal differences, with higher potential in the south in the current climate. In the  
36 future these differences where the current higher potentials in the south will diminish, while future as the potentials  
37 will increase in the north, especially for the summer grazing grounds. These combined results suggest significant  
38 shifts in vegetation composition over the present century for this scenario, with large implications for nature con-  
39 servation, reindeer husbandry and forestry.

40

## 41 **1 Introduction**

42 High-latitude regions harbour vast areas of relatively intact ecosystems, holding species of great ecological, ~~bio-~~  
43 ~~logical~~ and societal significance (Dobrowski et al., 2021). These northern ecosystems are predicted to be more  
44 vulnerable to climate change than most other terrestrial biomes (Hickler et al., 2012; IPCC, 2014). For each degree  
45 of global average ~~The observed~~ temperature increase, the observed increase in Fennoscandia has been estimated  
46 to be 2-3 degrees ~~per degree of global average increase~~ (Rantanen et al., 2022), and this relationship persists with  
47 persistent trends in future predictions (Ono et al., 2022). This temperature increase has strongly affected northern  
48 ecosystems, resulting in changing vegetation patterns in the Arctic (Elmendorf et al., 2012; Pearson et al., 2013),  
49 an overall taller plant community (Bjorkman et al., 2018) and increases in biomass (Hudson and Henry, 2009).  
50 The occurrence and distribution of shrubs has also been observed to increase, both in high latitude and high-  
51 altitude regions, as a result of the warmer climate (Elmendorf et al., 2012; Myers-Smith et al., 2011; Sturm et al.,  
52 2001). The distance species have to migrate to keep up with climate change is, however, shorter in alpine and  
53 Oroarctic regions than in flat boreal and Arctic landscapes (Feeley et al., 2011). As the boreal forest covers a wide  
54 area, its species composition and ability to provide ecosystem services could undergo large shifts, e.g. as a re-  
55 sponse to different disturbance patterns and hydrology changes (Venäläinen et al., 2020), even if its geographical  
56 extent is not changed. Consequences of future shifts in areal extent of vegetation zones, which may not be pro-  
57 portional to their current distributions, include reduced space of many habitats (Pauli and Halloy, 2019) and in-  
58 creased pressure on many species (Kuuluvainen and Gauthier, 2018).

59

~~The Fennoscandian boreal and Oroarctic region is located between 58 and 71 °N, spanning altitudes from sea  
60 level to 2469 m a.s.l. (Galdhøpiggen, Norway), and is characterised by continental to sub-oceanic climate  
61 (Oksanen and Virtanen, 1995). Boreal forest dominates from the coast towards the mountains up to latitude 68-  
62 69 °N. Above the boreal forest there is a zone of mountain birch forest which normally has a vertical distribution  
63 of ca 200 m. The tree line, formed by mountain birch, is in Sweden at an altitude of more than 1100 m in the south  
64 and decreases with latitude to 600 m in the north (Kullman, 2016). Above the tree line follows tundra with de-  
65 creasing levels of vegetation height and coverage (from shrub to barren tundra) and finally bare rocks and snow  
66 fields.~~

67

68  
69 In Fennoscandia, ~~the~~ herding of semi-domesticated reindeer is important in shaping this landscape, a practice  
70 which utilises the land from the coastal areas and the boreal forest in winter up to the tundra in summer (Käyhkö  
71 and Horstkotte, 2017). Reindeer grazing directly affects the vegetation composition and diversity, both in the  
72 mountains (Olofsson et al., 2001; Sundqvist et al., 2019; Vowles et al., 2017) and forested regions (Kumpula et

73 al., 2014). In summer, reindeer have a mixed diet of shrub leaves, forbs, herbs, sedges, grass, and fungal fruit  
74 bodies, and reindeer forage has been shown to reduce deciduous shrub expansion (e.g. Olofsson et al., 2001;  
75 Olofsson et al., 2009; Sundqvist et al., 2019; Vowles et al., 2017). In winter, reindeer mainly eat ground- and tree-  
76 lichens, which decreases ground-lichen cover (Kumpula et al., 2014). However, reindeer husbandry is currently  
77 experiencing increased pressure from human activities, such as forestry practices and tourism (Fohringer et al.,  
78 2021; Kumpula et al., 2014; Sandström et al., 2016), affecting 85% of the herding area (Stoessel et al., 2022). In  
79 addition, there are implications resulting from climate change, such as difficult snow conditions making winter  
80 forage hard (Rasmus et al., 2022; Rosqvist et al., 2021) and hot dry summers increasing heat stress (Käyhkö and  
81 Horstkotte, 2017). Climate change is increasing the pressure on both ecosystems and societies in these areas, a  
82 pressure that will increase in coming decades (Constable et al., 2022). Reindeer grazing and browsing can to some  
83 degree hold back the rate of tree-line advancement and tundra shrubification (Stark et al., 2023), but will not  
84 completely stop it. A future less open landscape will have a large impact on how reindeer graze and dwell in the  
85 landscape and on the Sami culture (Stark et al., 2023), but how that might affect the size of a sustainable reindeer  
86 population is hard to predict.

87  
88 Projections of future impacts of climate change in high latitude ecosystems can be made upon the implementation  
89 of understanding arising from empirical studies (e.g. Bjorkman et al., 2020; Myers-Smith et al., 2011) and remote  
90 sensing (e.g. Callaghan et al., 2022), into models such as dynamical vegetation models (DVMs) using climate  
91 model data as input. The typical cell size of a regional climate model (on the order of 10-50 km) often contains  
92 land surface types ranging from forest to bare rock or glaciers in mountainous areas. This information does not  
93 capture all local variation, especially in areas of complex terrain where altitudinal differences can be strongly  
94 underestimated (Lind et al., 2020). Also, while representing most meteorological processes some are only crudely  
95 implemented at such relatively coarse resolution in modelling studies (Lind et al., 2020). In recent years, one of  
96 these DVMs, LPJ-GUESS, have has been adapted to the boreal and Arctic regions (Miller and Smith, 2012; Wolf  
97 et al., 2008; Yu et al., 2017), and used with very highly resolved climate data (e.g. 50 × 50 m) have been used  
98 only at a local scale in sub-arctic Scandinavia (Gustafson et al., 2021; Tang et al., 2015). So far, however, no high-  
99 resolution (<10 km) study of environmental change and its impact on vegetation covering the entire Fen-  
100 noscandian boreal and Oroarctic region has been made.

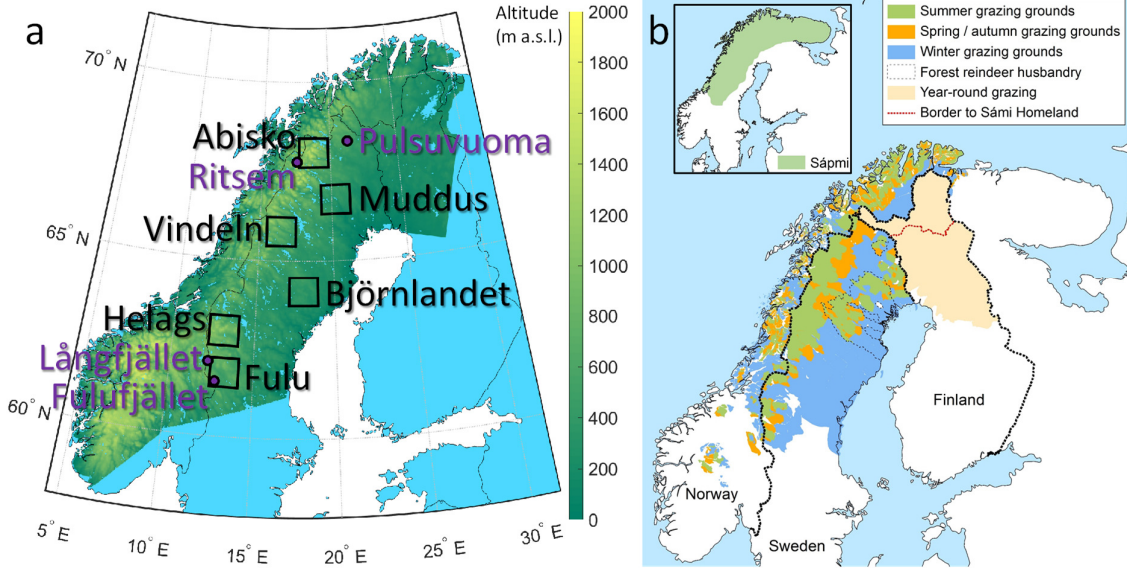
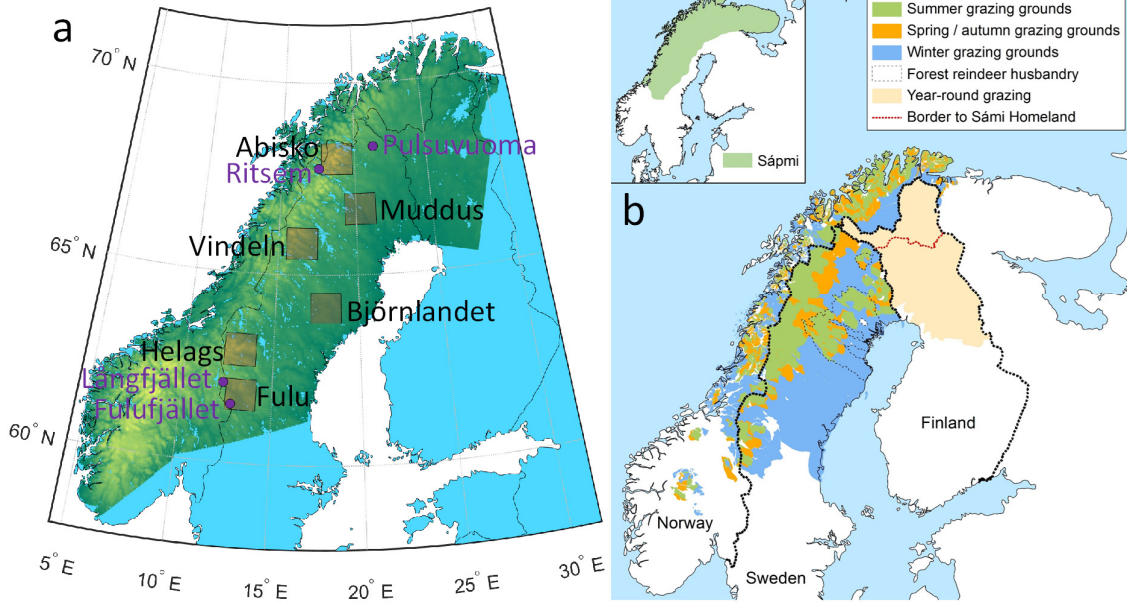
101  
102 Recently the first ever km-scale climate model projections at 3 km grid spacing were completed for the entire  
103 Fennoscandian region (Lind et al., 2020; Lind et al., 2022). Results from such km-scale simulations (1-4 km  
104 compared to previous coarser resolution >10 km), offer an unprecedented insight into weather and climate pro-  
105 cesses at high resolution, which is particularly important in complex terrain. In addition, it is important to under-  
106 stand how this improved weather and climate insights might affect vegetation dynamics and for that a DVM is  
107 needed. Thus, we here use this-these unique km-scale climate model projections for the high-emission RCP8.5  
108 scenario (Lind et al., 2022) and a-the state-of-the-art DVM; LPJ-GUESS (Lindeskog et al., 2021; Smith et al.,  
109 2001; Smith et al., 2014) (Smith et al., 2001; Smith et al., 2014), including a new module of reindeer grazing, to  
110 investigate the vegetation response to climate and environmental change in the Fennoscandian boreal and moun-  
111 tain regions used for reindeer herding. The results are validated against satellite products and field data gathered  
112 in the study region. Furthermore, we use consistent, high-resolution climate and nitrogen deposition scenarios to

113 evaluate potential future vegetation changes in the region, with a special emphasis on reindeer food supply and  
114 vegetation trends in “hotspot” areas with high biodiversity and conservation values. As the only available climate  
115 projection at this resolution is a high-emission scenario, the simulated state at the end of the century will provide  
116 a message to society of what to expect and plan for if emissions continue to increase. We hypothesize that this  
117 state will show extensive changes that will present challenges for forestry, reindeer herding, tourism and nature  
118 conservation, as the temperature increase is high in such a scenario

## 120 **2 Material and methods**

### 121 **2.1 Study area**

122 The study was restricted to the Fennoscandian mountain range and the adjacent boreal areas used for reindeer  
123 herding (Figure 1), with a focus on ecosystems in Sweden. The Fennoscandian boreal and Oroarectic  
124 is located between 58 and 71 °N, spanning altitudes from sea level to 2469 m a.s.l. (Galdhøpiggen, Norway), and  
125 is characterised by continental to sub-oceanic climate (Oksanen and Virtanen, 1995). Boreal forest dominates  
126 from the coast towards the mountains up to latitude 68-69 °N. Above the boreal forest there is a zone of mountain  
127 birch forest which normally has a vertical distribution of ca 200 m. The tree-line, formed by mountain birch, is in  
128 Sweden at an altitude of more than 1100 m in the south and decreases with latitude to 600 m in the north (Kullman,  
129 2016). Above the tree line follows tundra with decreasing levels of vegetation height and coverage (from shrub-  
130 to barren tundra) and finally bare rocks and snowfields. For a more detailed assessment of simulated changes, six  
131 “hotspot” areas (90 × 90 km) in the larger domain were selected to represent different vegetation zones with a  
132 high species richness and large conservation values, from the boreal forest to the high alpine tundra, and covering  
133 the entire Swedish mountain range (Table 1, Figure 1, Figure S1):



135

136

137 **Figure 1.** a) The study area (shown as altitude from sea level (dark green) to 2000 m a.s.l. (yellow), the six focus “hotspot”  
 138 areas (shaded squares and black text, see Figure S1 for detailed maps) and the four grazing exclusion sites (purple dots and  
 139 text). b) Map of grazing areas used for the semi-domesticated reindeer during different seasons in Norway, Sweden and Finland  
 140 (from Käyhkö and Horstkotte (2017), used with permission).

141

142 **Table 1.** Description of the six “hotspots”. Maps of the areas are shown in Figure S1.

Name	Coordinates	Type	Protected area	Description
Abisko	68° 01' N, 18° 46' E	Mountain	Abisko National Park, established 1909	Including the highest mountains (2097 m) in Sweden
Vindeln	65° 49' N, 16° 29' E	Mountain	Vindelfjällen Nature Reserve, established 1974	Including mountains reaching 1768 m

Helags	62° 58' N, 13° 06' E	Mountain	Vålådalen Nature Reserve, established 1988	Including the mountain Helags (1797 m)
Fulu	61° 47' N, 13° 17' E	Mountain	Fulufjället National Park, established 1973	At the southernmost part of the Scandes mountains (1196 m, Sömlinghågna) in Sweden
Muddus	66° 43' N, 20° 17' E	Forest	Muddus National Park, established 1942	Mostly boreal forest with extensive wetlands
Björnlandet	64° 07' N, 18° 01' E	Forest	Björnlandet National Park, established 1991	Boreal forest with some wetlands

143

## 144 2.2 Dynamical vegetation and ecosystem model

145 The dynamical vegetation and ecosystem model LPJ-GUESS\_(v4.1, Nord et al., 2021) (~~v4.1, Gustafson et al.,~~  
146 ~~2021; Smith et al., 2001; Smith et al., 2014~~) was used to simulate vegetation change in the region. Detailed de-  
147 scriptions of the development stages involves; first version (Smith et al., 2001), arctic development (Miller and  
148 Smith, 2012; Wolf et al., 2008), N-cycle (Smith et al., 2014), landcover (Lindeskog et al., 2021) and further arctic  
149 implementations (Gustafson et al., 2021). The model simulates the development of cohorts, belonging to different  
150 plant functional types (PFTs), when competing for light, nitrogen and water in replicate patches ~~representing an~~  
151 ~~area of ca 1000 m<sup>2</sup>~~ (here set to 15 patches per simulated climate gridcell). Each patch represents an area of ca  
152 1000 m<sup>2</sup>. The model includes detailed process descriptions related to the cycling of water (e.g. transpiration,  
153 evaporation, and snow and soil water dynamics), carbon (e.g. photosynthesis, respiration, fire, and allocation of  
154 biomass), and nitrogen (e.g. nitrification and restriction of photosynthesis), and is driven by temperature, radia-  
155 tion, relative humidity, wind speed, CO<sub>2</sub> concentration, and nitrogen deposition data. Except those that takes place  
156 in the soil, the processes are calculated at the cohort level. The PFTs are described by parameters related to growth  
157 form (tree, shrub or herbaceous), allocation, allometry, phenology, life history, shade tolerance and response to  
158 environmental and bioclimatic conditions. Patch destroying disturbances representing e.g. devastating pests or  
159 wind storms, occur randomly in each patch (~~the default v4.1~~ return time ~~set to of~~ 150 years ~~was used~~ in the pre-  
160 sented simulations). Separately, fire disturbance simulated with the BLAZE module (Molinari et al., 2021) was  
161 applied. A simulation starts after a spin-up period (set to 600 years) over which a detrended dataset comprising  
162 the first 30 years of historical climate data are repeated to get the vegetation in balance with the climate.

163

### 164 2.2.1 Plant functional types

165 In the present study, an expanded set of PFTs were used, which includes high-latitude PFTs such as shrubs, with  
166 separate sets for mineral and wetland soils~~for mineral soils, including high-latitude PFTs such as shrubs~~ (Table  
167 2). In each gridcell, the simulations on mineral and wetland soils are independent of each other.

168

169 **Table 2.** Plant functional types in the LPJ-Guess simulations. The last six PFTs were used for the wetland simulation and the  
170 rest for mineral soils.

PFT	Long name	Typical represented species
BNE	Boreal needle-leaved evergreen tree, shade tolerant	<i>Picea abies</i>

BINE	Boreal needle-leaved evergreen tree, shade intolerant	<i>Pinus sylvestris</i>
IBS	Shade-intolerant broadleaved summergreen tree	<i>Betula pubescens</i> ssp. <i>tortuosa</i>
TeBS	Shade-tolerant temperate broadleaved summergreen tree	<i>Fagus</i> , <i>Quercus</i> , <i>Fraxinus</i> spp
C3G	Cool (C3) grass	<u><i>Poaceae</i></u>
HSE	Tall shrub (up to 2m), evergreen	<i>Juniperus communis</i>
HSS	Tall shrub (up to 2m), summergreen	<i>Alnus incana</i> spp., <i>Salix</i> spp. e.g. <i>S. phyllifolia</i> and <i>S. myrsinifolia</i> , <i>Betula nana</i>
LSE	Low shrub (up to 0.5m), evergreen	<i>Vaccinium vitis-idaea</i> , <i>Empetrum</i> spp.
LSS	Low shrub (up to 0.5m), summergreen	<i>Vaccinium myrtillus</i> , small <i>Salix</i> spp. e.g. <i>S. arbuscula</i>
GRT	Graminoid and forb tundra	Grass, sedge and forb tundra species
EPDS	Evergreen prostrate (up to 0.2m) dwarf shrubs	<i>Vaccinium oxycoccos</i> , <i>Cassiope</i> spp., <i>Dryas octopetala</i> , <i>Saxifraga</i> spp.
SPDS	Summergreen prostrate (up to 0.2m) dwarf shrubs	Dwarf <i>Salix</i> spp. e.g. <i>S. herbacea</i> , <i>Arctostaphylos alpinus</i>
CLM	Cushion forb, lichen and moss tundra	<i>Saxifragaceae</i> , <i>Caryo-phyllaceae</i> , <i>Draba</i> spp., lichens, mosses
pLSE	Peatland low shrub, evergreen	<i>Vaccinium vitis-idaea</i> , <i>Cassiope</i> spp.
pLSS	Peatland low shrub, summergreen	<i>Vaccinium myrtillus</i> , <i>V. uliginosum</i> , <i>Salix hastata</i> , <i>S. glauca</i>
pCLM	Peatland cushion forb, lichen and moss tundra	<i>Saxifragaceae</i> , <i>Caryophyllaceae</i> , <i>Papaver</i> spp., <i>Draba</i> spp., lichens, mosses
WetGRS	Cool, flood-tolerant (C3) grass	<i>Carex</i> spp., <i>Eriophorum</i> spp., <i>Juncus</i> spp., <i>Typha</i> spp.
pmoss	Peatland moss	<u><i>Spagnum</i> e.g. <i>S. fuscum</i></u>
C3G_wet	Peatland cool (C3) grass	<u><i>Poaceae</i></u>

171

172 For fractions of land classified as peatland, we use a version of the model with peatland integration (Wania et al.,  
173 2009a, b), which include a wetland hydrology module and wetland PFTs (Miller and Smith, 2012; Wolf et al.,  
174 2008; Zhang et al., 2013). The fractions of mineral soil and wetland were prescribed and constant over the simu-  
175 lation period based on the PEATMAP product at a 0.125° (14 km in S-N direction and 5-7 km in W-E direction  
176 depending on latitude within the assessed area) resolution (Xu et al., 2018). Weighted averages of model results  
177 were calculated based on these fractions. ~~Test runs showed underestimation in the spatial extent of~~For the shade-  
178 intolerant broadleaved summergreen tree (IBS) PFT some parameters were changed according to Gustafson et al.  
179 (2021) in an application for Abisko, Sweden. Their revision was made to reflect the fact that this global PFT in  
180 Fennoscandia mainly, which represents ~~the~~ mountain birch (*Betula pubescens* ssp. *tortuosa*) ~~forest that normally~~  
181 forms the tree line in Fennoscandia. Details of the IBS parameterization are found in .A fine tuning of some of  
182 the model's parameters was therefore done to get a better match against distribution maps from observations  
183 (Table S2).

184

### 185 2.2.2 Reindeer grazing, browsing and trampling

186 To simulate the effect of reindeer grazing, browsing and trampling, a new module was added to the model. Graz-  
187 ing/browsing was simulated by removing a fraction of leaf biomass. The model only includes stem and leaf as

188 above-ground compartments. We note however that when browsing reindeer also consume tops, twigs and branch  
189 biomass, which mean that we may underestimate the effect on vegetation, but to keep the model uncomplicated  
190 this simplification was applied. Trampling was simulated by killing a fraction of the individuals in a cohort, or, in  
191 the case of herbaceous PFTs, a fraction of total biomass. The grazing/browsing and trampling level was based on  
192 a constant intensity of herbivory. For a specific PFT, the grazing/browsing was determined by a preference value  
193 obtained from extensive observations of the feeding preferences of semi-domesticated reindeer in Canada  
194 (Denryter et al., 2017) and if the cohort's canopy height was within reach of reindeer. The sensitivity to trampling  
195 was based on the vegetation response in an artificial trampling experiment (Egelkraut et al., 2020). All the con-  
196 sumed carbon in the leaves was treated as harvested but only a fraction of the leaf nitrogen. The other fraction of  
197 the consumed N was added to the cohort's leaf N pool, which reflects the assumption that N leaving the herbivore  
198 as urine is directly-rapidly taken up by the plants (Barthelemy et al., 2018). A detailed description of the module  
199 and its parameter values is given in S3. From this module, the resulting output of consumed C biomass was used  
200 as an indicator of potential reindeer food consumption. In the presented simulations, the simulated grazing, brows-  
201 ing and trampling in a patch was set to have a return time of 3 years (see S3 for motivation), a grazing intensity  
202 of 0.1 (fraction yr<sup>-1</sup>), a max height of 2.5 m and that 35% of browsed nitrogen (Ferraro et al., 2022; Mcewan and  
203 Whitehead, 1970) was removed to the harvest pool.

### 205 **2.3 Model input data: climate**

206 The regional climate modelling system HCLIM38 (Belušić et al., 2020) was used for downscaling the RCP8.5  
207 scenario simulation from the global climate model EC-Earth (Hazeleger et al., 2010; Hazeleger et al., 2012). The  
208 climate scenario was first downscaled to 12 km with HCLIM38-ALADIN (Belušić et al., 2020) for the period  
209 1985-2100 and then further to 3 km with HCLIM38-AROME (Belušić et al., 2020) for the periods 1985-2005,  
210 2040-2060 and 2080-2100 (Lind et al., 2020; Lind et al., 2022). For computational reasons we wanted to restrict  
211 the size of the complete 1985-2100 NetCDF climate files to less than 32 GB per climate variable. Therefore, a cut  
212 of the original data was made at the south, north and west Norway-mainland limits as well as an eastern border  
213 through the north of Finland (Figure 1).

214  
215 The years 1985 in the ALADIN 12 km data and 1985, 2040 and 2080 in the AROME 3 km data were spin-up  
216 years. To test the robustness of the results, all climate variables used by the vegetation model were also compiled  
217 ~~(see below)~~ without using the HCLIM spin-up years and tested on a sub-set of 200 random gridcells. As there  
218 were no significant differences in the results we present results based on climate data including the HCLIM spin-  
219 up years.

220  
221 For filling the periods when only ALADIN data were available, we first produced datasets ~~were first made~~ such  
222 that the four AROME gridcells coinciding with a certain ALADIN gridcell were filled with data from that ALA-  
223 DIN gridcell (termed ALAatARO, 1985-2100). The periods with missing 3-km AROME data were filled with the  
224 ALAatARO data using two methods:  
225



226 For precipitation, global radiation, relative humidity, and wind speed, linear regressions through origin for the  
227 overlapping periods between AROME data and the ALAatARO data were used. The relations were fitted sepa-  
228 rately by month and, specifically, data from 1985-2005 and 2040-60 were used to establish the relationships for  
229 the 2006-2039 period, and 2040-2060 and 2080-2100 for the 2061-2079 period. The relationships were then used  
230 to get 3-km data for the missing periods from ALAatARO data.

231

232 For daily, minimum and maximum temperatures a non-parametric empirical quantile mapping “QUANT” bias  
233 correction method (e.g. Osuch et al., 2017) was applied by month using daily temperature data for 21-year periods.  
234 Two reference periods were used with observed  $1 \times 1$  km data from Nordic Gridded Climate Dataset (NGCD,  
235 [https://surfobs.climate.copernicus.eu/dataaccess/access\\_ngcd.php](https://surfobs.climate.copernicus.eu/dataaccess/access_ngcd.php)) that were aggregated to the AROME grid,  
236 1985-2005 (used for AROME grid data) and 1998-2018 (used for ALAatARO grid data). In the quantile mapping,  
237 intervals of 1% were applied and a smoothing was done using a running mean over 5 intervals. Modelled and  
238 matching observed values were linearly interpolated between the intervals. For consistency, all calculations of  
239 quantiles were done for 21-year periods, resulting in an overlapping period (1998-2005) for which the AROME  
240 data were used. For the future, the difference between observed and scenario quantiles during the reference period  
241 was added to the matching quantile of future 21-year periods. The future periods were 2040-2060 and 2080-2100  
242 for the AROME data and 2019-2039 and 2060-2080 (2060 and 2080 not used) for the ALAatARO data.

243

244 The RCP8.5 scenario used was the first dataset produced at this high resolution for the entire region. It is a scenario  
245 with strongly increasing emissions of greenhouse gases, but the projection up to the mid-century is similar to  
246 lower emission scenarios (Meinshausen et al., 2011). In the resultant daily air temperature data, the climate-change  
247 signal was a 1.0-2.3 K increase in mean annual temperature from the 1991-2020 to the 2031-2060 30-year periods,  
248 and a 2.5-5.2 K increase from 1991-2020 to 2071-2100 (Figure S4a-b). For annual precipitation the relative change  
249 was -2.3 – 23.1% to 2031-2060 and -0.9 – 50.1% to 2071-2100 (Figure S4c-d).

250

#### 251 **2.4 Model input data: soil texture, atmospheric nitrogen deposition and CO<sub>2</sub>**

252 Soil texture data (clay and sand fraction) at 3 km resolution were taken from SURFEX (Masson et al., 2013), the  
253 land surface model of AROME, ensuring consistency with LPJ-GUESS. These data originate from FAO soil  
254 texture data at ~~50.0833° – are seconds – (40–9 km in S-N direction and 3-5 km in W-E)~~ resolution  
255 (<https://data.apps.fao.org/map/catalog/static/search?keyword=DSMW>) ~~that had been interpolated to 3 km resolu-~~  
256 ~~tion.~~

257

258 Nitrogen deposition at monthly temporal resolution was used as input to LPJ-GUESS. The input was based on  
259 two model simulations (MATCH-BIODIV and MATCH-ECLAIRE) with the Multi-scale Atmospheric Transport  
260 and Chemistry (MATCH, Andersson et al., 2015; Andersson et al., 2007; Robertson et al., 1999) model. MATCH-  
261 BIODIV (Andersson et al., Manuscript; Eichler et al., 2023) was forced by the climate simulation ALADIN at 12  
262 km, and anthropogenic air pollution emissions from ECLIPSE V6b (Höglund-Isaksson et al., 2020). This data set  
263 (<https://previous.iiasa.ac.at/web/home/research/researchPrograms/air/ECLIPSEv6b.html>, accessed Feb 2020) has  
264 a resolution of 12 km and covers the period 1987-2051. MATCH-ECLAIRE (Engardt et al., 2017) was constructed

265 at 50 km resolution for 1900-2050, based on current climate and varying anthropogenic air pollutant emissions  
266 ECLIPSE V4a and Lamarque et al. (2010).

267

268 MATCH-ECLAIRE was used to obtain 12 km resolution nitrogen deposition fields for the time period 1900-  
269 1986. This was done by establishing a linear relationship through zero for the overlapping period for each  
270 MATCH-BIODIV and MATCH-ECLAIRE gridcell and subsequently applying it to downscale the 50 km data  
271 for the 1900-1986 period. After 2051, the 0.5° (56 km in S-N and 18-29 km in W-E) resolution Lamarque et al.  
272 (2011) dataset was used, which is standard for LPJ-GUESS. A sensitivity test for a selection of gridcells showed  
273 very minor differences when comparing modelling results for simulations using the different resolution of N dep-  
274 osition data (results not shown), from which we concluded that this simplification was justified.

275

276 The future trend in nitrogen deposition is similar for MATCH-BIODIV and MATCH-ECLAIRE, i.e. declining  
277 until mid-century. The modelled total deposition in the Scandinavian Mountain area is dominated by oxidized  
278 nitrogen, which exhibits a clear decline, while reduced nitrogen deposition levels off at around 2020 and after that  
279 even increases slightly for MATCH-BIODIV. These data sets have been evaluated against reanalysis data con-  
280 sisting of fused observations and modelled estimates (Andersson et al., Manuscript) for years where all datasets  
281 were overlapping (1987-2013) for high-altitude areas of the Scandinavian Mountains. The comparison shows a  
282 positive bias in the quantitative modelled total nitrogen deposition by 18% and 23% respectively for the 1987-  
283 2013 period, with a stronger positive bias in oxidised nitrogen deposition and a partly balancing negative bias in  
284 reduced nitrogen. The trend is similar between the modelled and the reanalysed datasets over the period.

285

286 Historical and RCP8.5 CO<sub>2</sub> concentration data were the same as used by EC-Earth and HCLIM38, reaching at-  
287 mospheric concentrations of 540.5 ppm and 935.9 ppm in 2050 and 2100, respectively (IPCC, 2013).

288

## 289 **2.5 Model output validation and analysis**

290 The output data from LPJ-GUESS are given as yearly states or sums of fluxes averaged over the 15 simulated  
291 patches. The data were further averaged over 10-year periods to reduce fluctuations arising from interannual  
292 weather variability and random disturbances.

### 293 **2.5.1 Validation**

294 The simulated total leaf-area index (LAI) was compared to yearly maximum of the monthly SURFEX LAI product  
295 (Masson et al., 2013), taken from ECOCLIMAP2.2 based on MODIS at 1 km resolution in 2000 (Faroux et al.,  
296 2013). Further, The modelled LAIs for the different-specific PFTs within a gridcell were used to determine was  
297 also converted, to be able to compare, to vegetation classes for comparison to two remote-sensing based vegetation  
298 products: the land cover of northern Eurasia (GLCE) based on SPOT 4 at 1 km resolution (Bartalev et al., 2003)  
299 and the CLC2018 Corine land-cover dataset (Corine) based on Sentinel 2 at 100 m resolution ([https://land.coper-](https://land.copernicus.eu/pan-european/corine-land-cover/clc2018)  
300 [nicus.eu/pan-european/corine-land-cover/clc2018](https://land.copernicus.eu/pan-european/corine-land-cover/clc2018)). The conversions (described in detail in S5) were based on  
301 Bartalev et al. (2003) and Kosztra et al. (2019) for GLCE and Corine, respectively. The satellite-based products  
302 were aggregated to the 3 km AROME gridcells, based on dominant class, to enable a statistical analysis of the

303 agreement by means of confusion matrixes (e.g. Congalton, 1991), with the satellite products used as ground truth.  
304 Three measures of accuracy were calculated. Producer accuracy (PA, probability that a value in a given class was  
305 classified correctly, i.e. correctly predicted gridcells of a class / total number of ground truth gridcells in that  
306 class), and user accuracy (UA, probability that a value predicted to be in a certain class really is that class, i.e.  
307 correctly predicted gridcells of a class / total number of gridcells predicted to be in the class) were calculated for  
308 each vegetation class, as well as the overall accuracy (sum of all correctly classified gridcells for all classes / total  
309 number of gridcells).

310

311 The model output was also evaluated against ground-based data for biomass (trees and shrubs) and vegetation  
312 coverage (field-layer) using data collected in 2011-2012 from four long-term enclosure experiments at Pulsu-  
313 vuoma, Ritsem, Långfjället and Fulufjället (for Ritsem only field-layer coverage), all established in 1995 (Figure  
314 1a) (Eriksson et al., 2007; Vowles et al., 2017). At each site and vegetation type (birch forest or shrub heath) there  
315 were three fenced enclosure plots and three ambient plots of dimension 25 × 25 m. For the gridcells corresponding  
316 to these experiments, the model was run both with a) continuous grazing and b) grazing stopped after 1995. To  
317 convert model-simulated total biomass C to dry mass, a factor of 2.0 was used (Thomas and Martin, 2012), and  
318 to convert modelled total biomass to above ground biomass we assumed a factor of 0.85 based on earlier estimates  
319 for Swedish birch forest (between 0.79 and 0.92, Johansson, 2007). For seedlings, Huttunen et al. (2013) reported  
320 values of about 0.6 increasing to 0.7 with fertilization and elevated temperature, but seedlings in general have  
321 lower above-ground fraction. (Qi et al., 2019). The vegetation cover data of the shrub and field layer, visually  
322 estimated at species level, were aggregated to the LPJ-GUESS PFTs and compared to simulated LAI for 2-3 close  
323 gridcells with similar altitude. Though the comparison of fractional plant cover and LAI is not strictly direct, the  
324 two measures are closely related (George et al., 2021).

325

## 326 2.5.2 Analysis

327 Due to the more detailed adapted vegetation zones for boreal and Arctic conditions in the GLCE classification,  
328 compared to Corine, the future trends presented in the results below focus only on the GLCE data.

329

330 To assess the simulated vegetation diversity, the Shannon (1948) Diversity Index ( $D$ ) was calculated for each of  
331 the six “hotspots” (Fig. 1) letting the number of gridcells of different vegetation classes represent diversity:

$$332 D = -\sum(p_i \times \ln(p_i)) \quad (1)$$

333 Where  $p$  is the fraction of the total numbers of classified gridcells in the “hotspot” (excluding prescribed water  
334 and wetland cells) belonging to class  $i$ . Only one vegetation class present would give a  $D$  of 0 and ten classes with  
335 the same  $p$  would give a value of 2.3.

336

337 The simulated potential reindeer consumption of leaf carbon was aggregated to reindeer herding communities in  
338 Sweden for traditional seasonal grazing grounds (Figure 1b), with help of GIS data obtained from the Swedish  
339 Sami Parliament ([www.sametinget.se](http://www.sametinget.se)).

340

## 341 2.6 Biodiversity data

342 To investigate the sensitivity of the “hotspot” sites to change, species observations of all available species groups  
343 together with threatened and red listed species, were extracted for each hotspot area using a GeoJSON file in the  
344 “The Analysis portal for biodiversity data” database (downloaded 29<sup>th</sup> of October 2021. <https://www.analysisportal.se/>). Further, to identify species being classified as alpine, the database “artfakta” (<https://artfakta.se/rodlistan>)  
345 was used with selection criterion “Landscape type” set to “Mountainous”.  
346  
347

## 348 3 Results

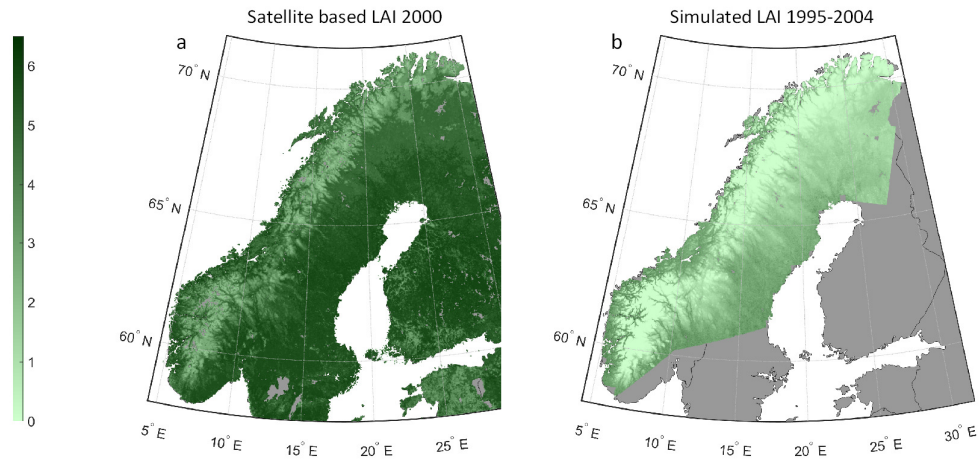
### 349 3.1 Validation

#### 350 3.1.1 Validation of simulated vegetation against satellite-based products

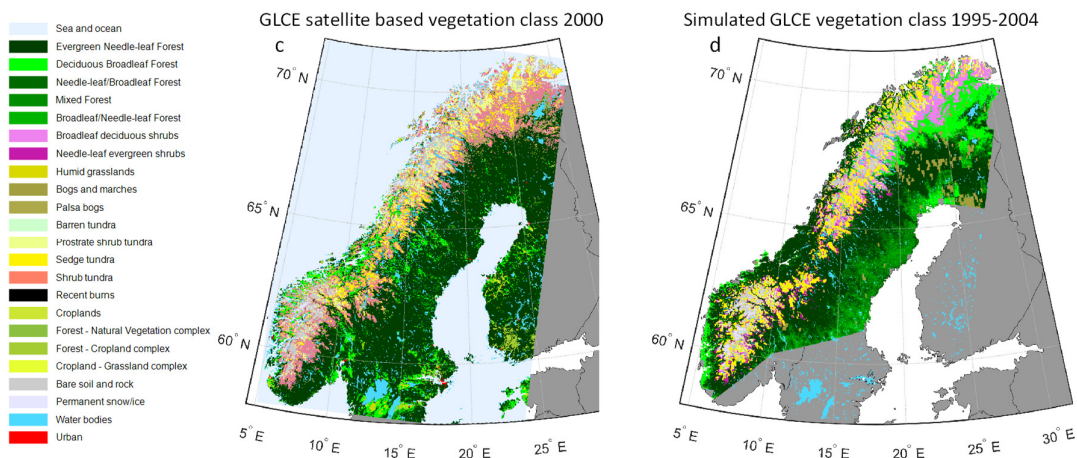
351 Simulated LAI was substantially lower than in the satellite based SURFEX product but had a reasonable agree-  
352 ment (Figure 2a-b, Simulated\_LAI =  $0.78 \times \text{SURFEX\_LAI} - 1.99$ ,  $r^2 = 0.59$ ). A reason for the low simulated  
353 values compared to the reference could be that yearly maximum of the SURFEX data were used, which can cause  
354 an overestimation if there are errors in the monthly data. Another aspect is that LAI is defined as one sided for  
355 SURFEX and projected in LPJ-GUESS, which corresponds to a factor of about 1.35 for needle leafed canopies  
356 (Flower-Ellis and Olsson, 1993).  
357

358 The simulations capture most of the broad patterns seen in the vegetation distribution from forest to non-vegetated  
359 areas when compared to the satellite-based products in 2000 and 2018 (Figure 2c-f). For the detailed classes of  
360 the GLCE map the overall accuracy is however only 32% of the gridcells (Table S6a) and for the somewhat wider  
361 classes of Corine 37% (Table S6b). Classifying in broader classes, the extent of forest agreed for 84% of gridcells  
362 simulated to be forest for both GLCE and Corine (user accuracy, UA) and for 90% and 94% of the satellite-based  
363 forest gridcells (producer accuracy, PA) for GLCE and Corine respectively. The most common class of the boreal  
364 forest, the needle leaved evergreen forest class, is more mixed with broad-leaved trees in the simulation and the  
365 distribution west of the mountains is overestimated compared to the satellite-based products. With the new para-  
366 metrization of the IBS PFT (Table S2), the deciduous broad-leaved forest expands too much in the north on the  
367 east side of the mountain ranges. Many (30%) of the gridcells that have shrub tundra according to the satellite  
368 data were classified as shrub vegetation, resulting in poor UA for broad-leaf deciduous shrubs (0.5%) and needle-  
369 leaf evergreen shrubs (0.0%), and poor PA for shrub tundra (0.2%) and PA for those classes in the GLCE com-  
370 parison. The classes are distinguished based on if the LAI of trees and tall shrubs is more than 20% of the total  
371 LAI (Figure S5b). Similarly, for Corine the simulated transitional woodland-shrub class mainly coincides with  
372 gridcells classified as broad-leaved forest, moors and heathland, and sparsely vegetated by the satellite product  
373 (Figure S5a).  
374

375



376



377

378

379

380

**Figure 2.** Satellite -based products of LAI (a), GLCE vegetation classes (c), and Corine vegetation classes (e) compared to simulated total LAI (b) and vegetation classes based on LAI averaged over 10-year periods for different PFTs according GLC Northern Eurasia (d) and Corine (f) (see Figure S5a-b).

381

382

383

Aggregating the tundra classes for GLCE gave a UA of 83% and PA of 36%, where the low PA is the result of many gridcells classified as shrub tundra by the satellite data being simulated to be forest or shrub vegetation. The

384 “moors and heathland” class is the third largest in the Corine satellite data and was often classified as forest,  
385 natural grassland or transitional woodland-shrub by the simulation (UA 18%, PA 4%). The LAI limit for the  
386 definition of the bare rock and glacier classes from the simulation were the same for GLCE and Corine classifi-  
387 cation and both classes were reduced in abundance from 1995-2004 to 2013-2022. The UA and PA for these  
388 classes were in the range 11-57%.

389

390 **3.1.2 Effect-Validation of the effect of the new reindeer module against vegetation inventories and reindeer**  
391 **exclosures**

392 Comparing model data and the *in-situ* estimated biomass for the northernmost Pulsuvuoma site showed that sim-  
393 ulated tree and shrub biomass was underestimated by ca 35% but was within the inventoried uncertainty range of  
394 the exclosure site (Figure 3). For the southern sites, biomass was overestimated by ca 50% at Långfjället and by  
395 200% at Fulufjället. A reason for the substantial overestimation for Fulufjället is that it was dominated by needle-  
396 leaf trees in the simulation. This was confirmed by test simulations; excluding pine and spruce PFTs (BINE and  
397 BNE) reduced biomass with 14%, excluding also the birch PFT (IBS) reduced biomass with 78%.

398

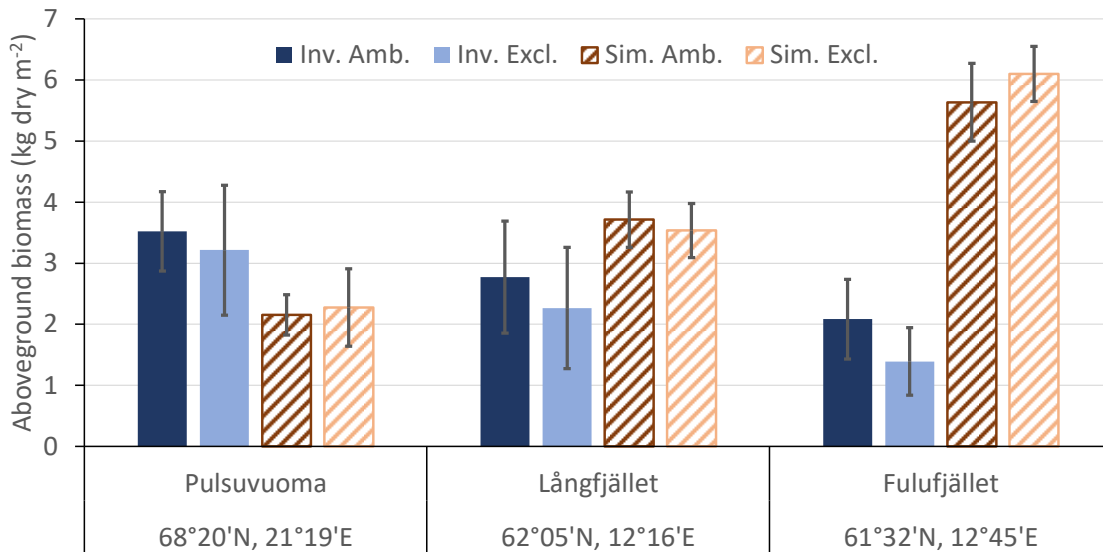
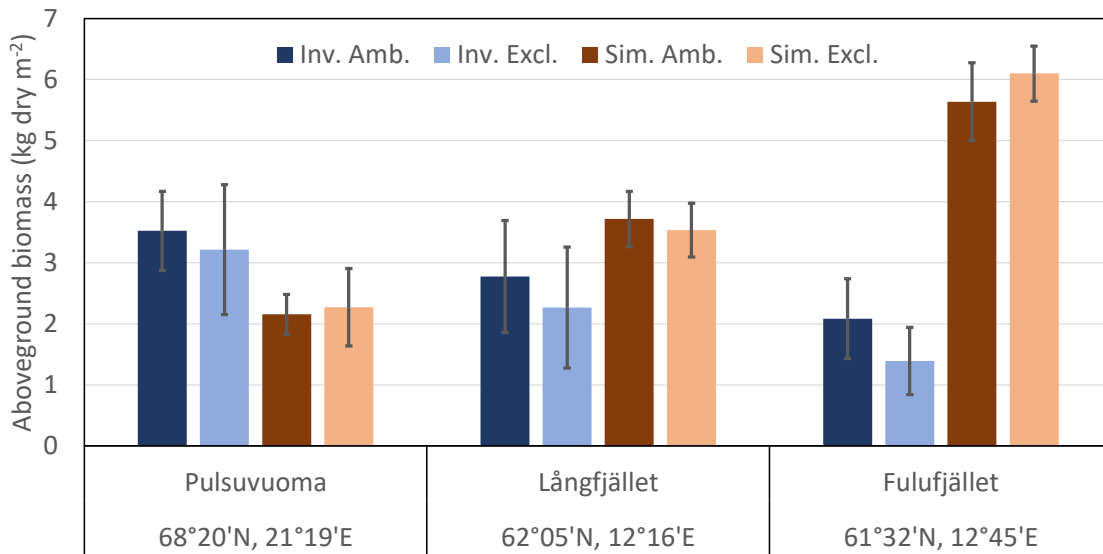


**Figure 3.** Simulated (Sim., mean over years 2009-2013, dashed bars) aboveground tree and shrub biomass compared to inventoried data (Inv. 2011 or 2012, solid bars, no biomass data were available for the Ritsem exclusion site) from experiments with ambient plots (Amb., dark bars) with reindeer access and plots with exclusion from 1995 (Excl., bright bars). Average and standard deviation over 3 inventoried plots or the 2-3 closest simulated gridcells.

The *in-situ* observed coverage of the shrub and field layer from the four exclusion sites was dominated by low evergreen shrubs, mainly *Calluna vulgaris*, *Empetrum nigrum* and *Vaccinium vitis-idaea*, except for the Ritsem shrub heath, which was dominated by graminoids and herbs (Figure S6). The total simulated LAI of the shrub and field layer was low for the two northern sites (0.08 to 0.26 compared to inventoried coverage of 59-75%) and was dominated by graminoids and herbs in the Ritsem shrub heath and high summer-green shrubs below the Pulsuvuoma birch forest. There was a trend that exclusion from reindeer grazing decreased the abundance of graminoids and herbs in both observation and simulations. For the two southern sites, the inventoried coverage and simulated

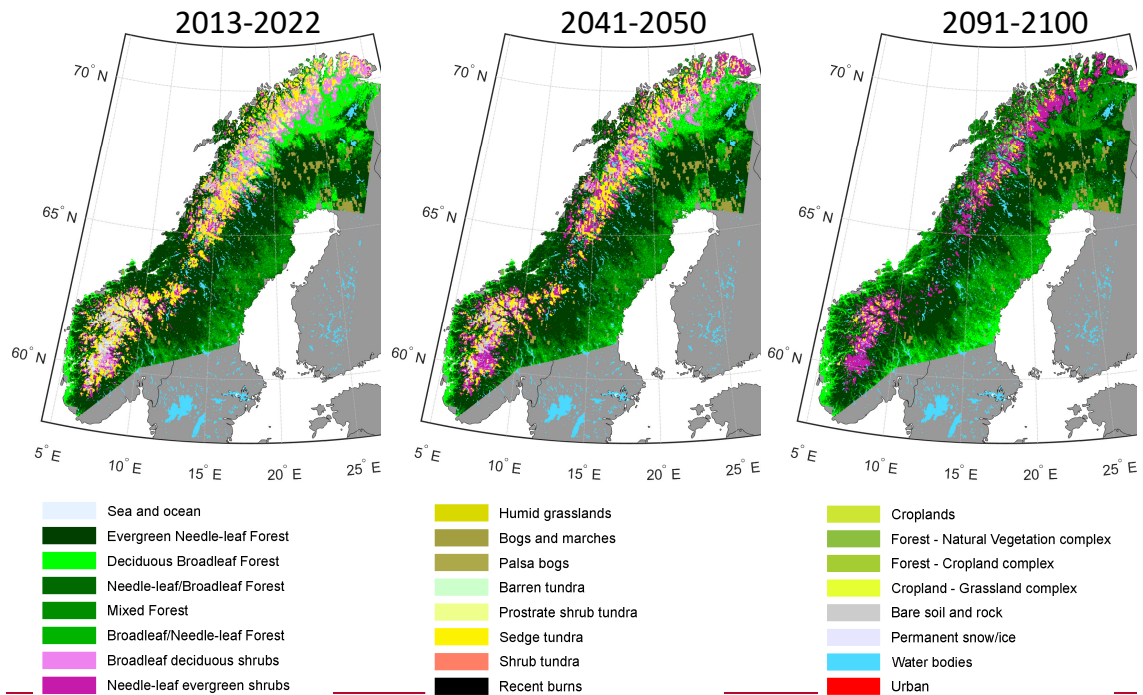
414 LAI were similar except for Fulufjället, which had a simulated overstory of denser evergreen conifers instead of  
 415 birch. The trends after exclosure are less clear for the southern sites and the short shrub classes that dominate in  
 416 the inventories are almost totally absent in the simulations, which are dominated by high shrubs (up to 2m tall),  
 417 graminoids and herbs. It should be noted that Fulufjället is located outside the area used for reindeer herding,  
 418 though it is occasionally visited by reindeers from Norway and moose, and the modelling case is hypothetical.  
 419

420 **3.2 Simulations and analysis of trends in vegetation 2000-2100**

421 **3.2.1 Trends in simulated vegetation classes over the whole simulated area**

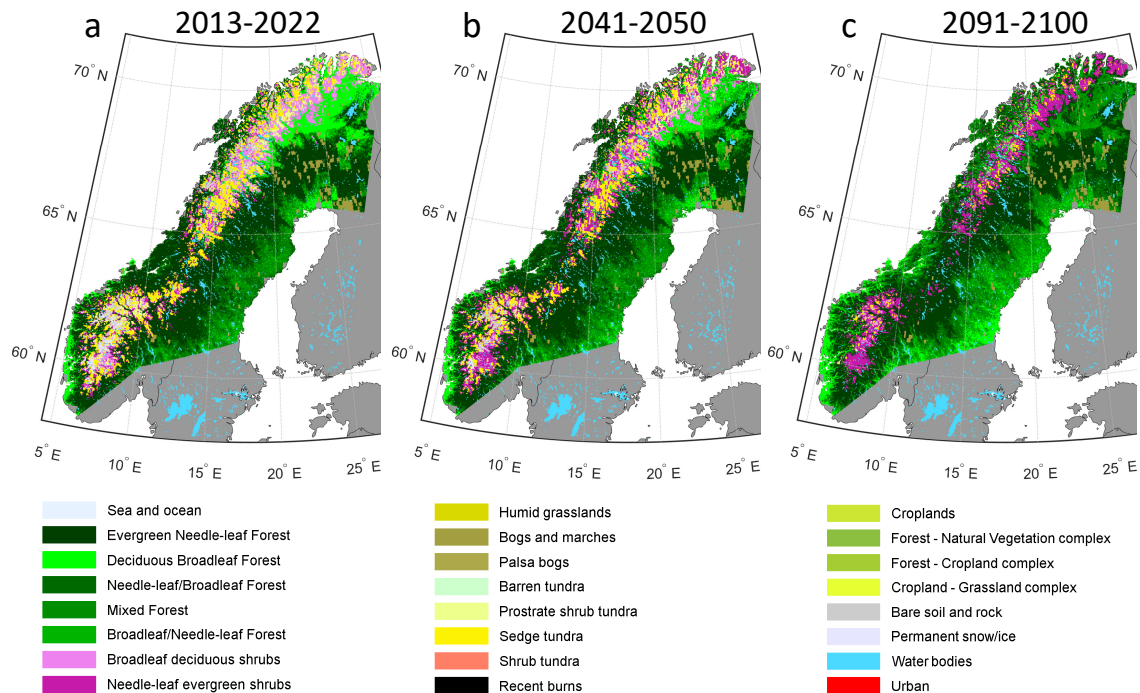
422 In the RCP8.5 scenario a dramatic shift in simulated vegetation composition was found, especially after 2050  
 423 (Figure 4). By 2041-2050 the shrub vegetation classes are already seen to expand to higher elevations in the  
 424 mountains and the broad-leaved forests in the north start to be mixed with conifers. At the end of the century, the  
 425 simulated area coverage of open vegetation classes and the barren-bare soils and rock class were was found to be  
 426 negligible. For instance, the Fennoscandian Low Arctic tundra, which stretches like a wedge from the Kola Pen-  
 427 insula to northernmost Swedish Lapland, in the lee of the mountain chain, would be completely lost by 2100  
 428 (Figure 4c). Along the southern part of the Norwegian coast and the south-eastern part of the Swedish boreal  
 429 forest, temperate broadleaf trees (TeBS PFT) start to become dominant in the 2091-2100 period, shown by in-  
 430 creasing areas of the deciduous broadleaf class.

431



432





433

434

**Figure 4.** Simulated vegetation classes according to the GLC Northern Eurasia classification based on average LAI for different PFTs over ten years, for three periods (a-c) in the RCP8.5 scenario.

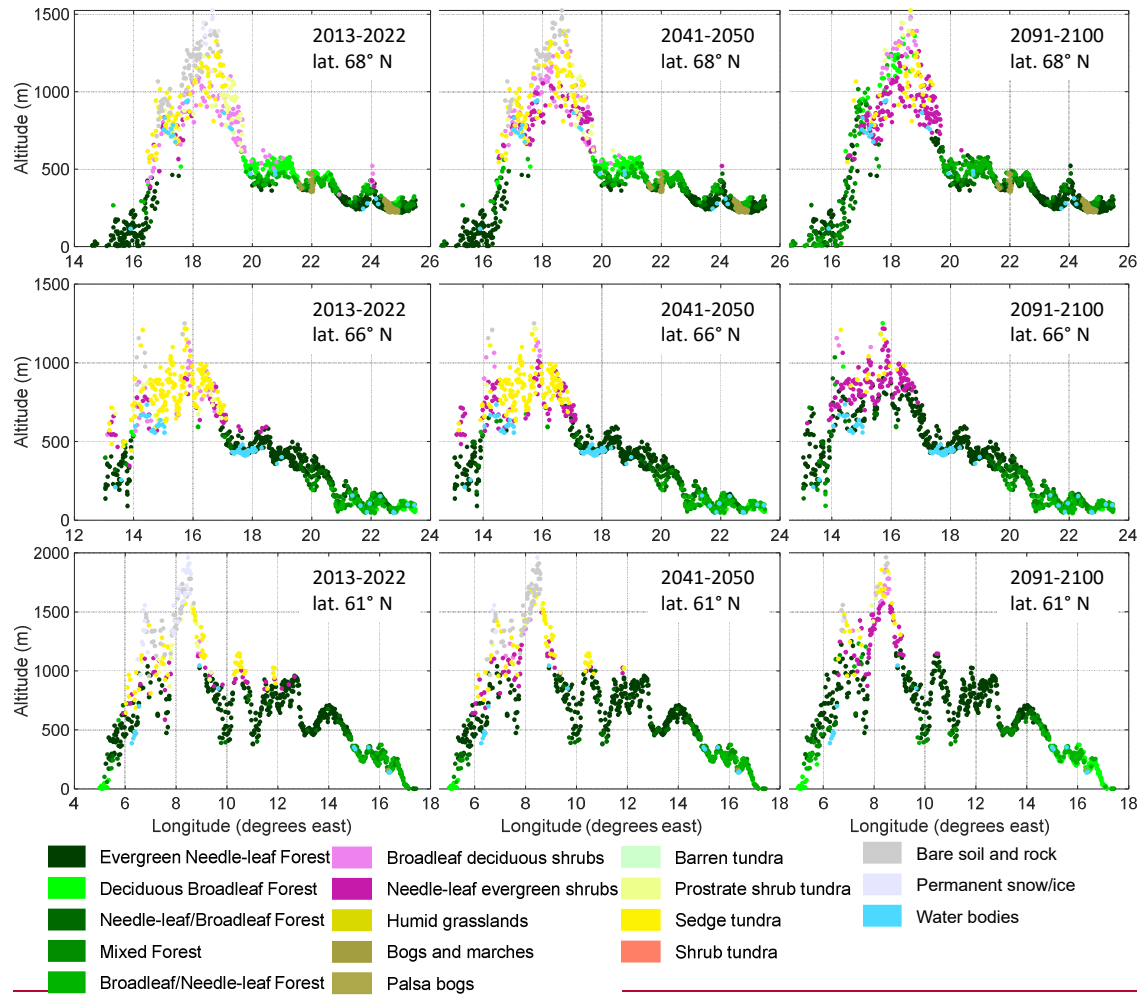
435

436

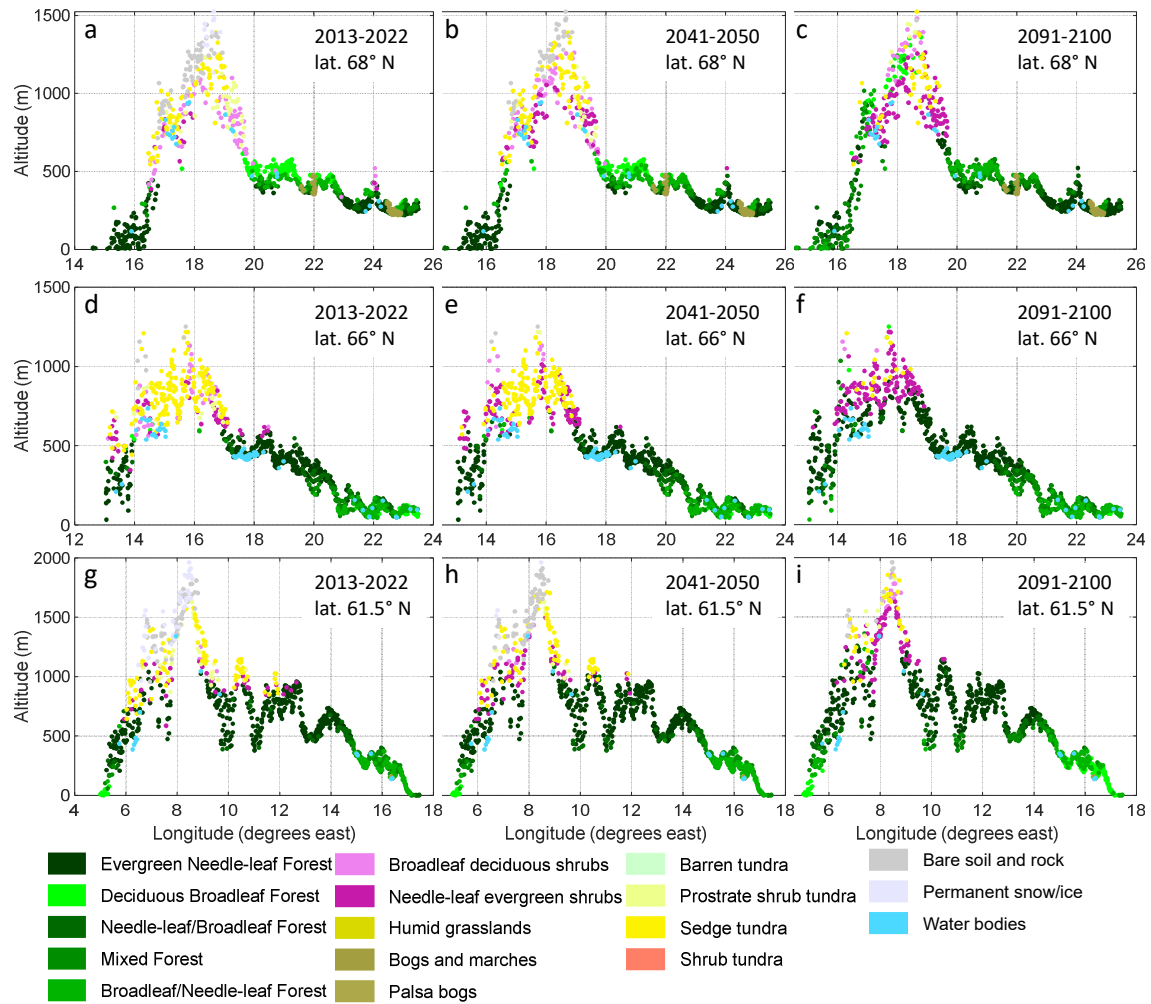
437

In the western part of the mountains at latitude  $68^{\circ}$  N, deciduous and mixed forests advance from a simulated current maximum altitude of ca 500 m a.s.l. to more than 1200 m in 2090-2100 (Figure 5a-c). On the east side there is no altitudinal advancement of the forest but a shift from deciduous broad-leaved trees to conifers. Shrub vegetation classes, especially needle-leaved shrubs, become dominant at mid to high altitudes, for  $66^{\circ}$  N (Figure 5d-f) and  $68^{\circ}$  N at about 700 to 1200 m and for  $61.5^{\circ}$  N less distinctly at 1000 to 1700 m (Figure 5g-i). At latitude  $61.5^{\circ}$  N, the lower mountains east of the mountain range become almost completely covered by evergreen needle-leaf forest. The changes seen in the 2041-2050 period are less distinct but the increase in needle-leaved shrubs has started by then, and in the highest elevations a shift in gridcell classification from permanent snow/ice to bare rock can be seen, indicating continued melt of glaciers and snowfields. As the classification is based on LAI, bare rock was set for LAI 0.01-0.001 and permanent snow/ice  $< 0.001$  see S5, it indicates that plants have the potential to grow there.

448



449



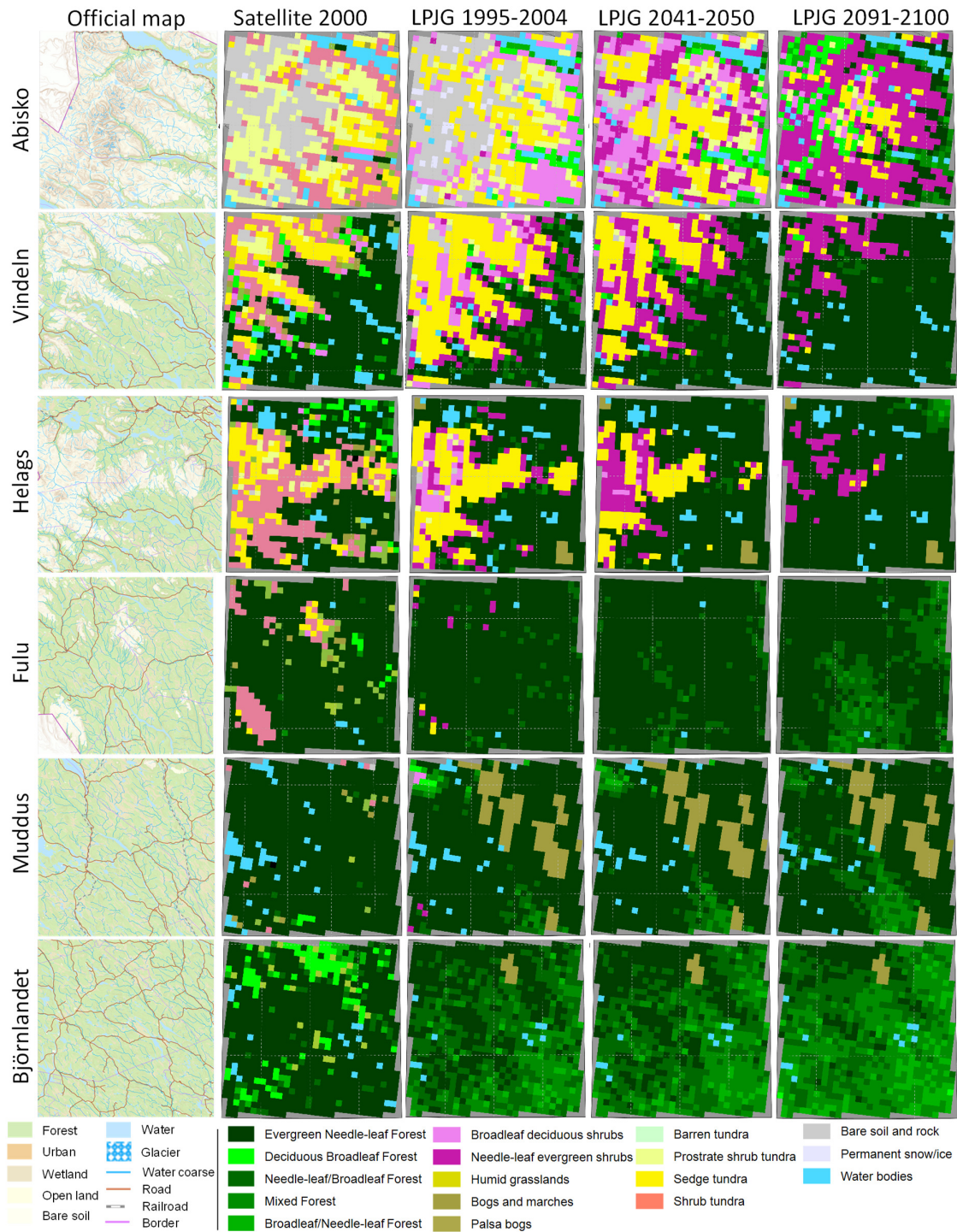
450

451 **Figure 5.** Profiles of simulated vegetation class according to GLCE for the 2013-2022 and RCP8.5 2041-2050 and 2091-2100  
 452 time periods, shown at the gridcells' longitude and altitude for three latitude bands at: 68.0-68.2° N (a-c), 66.0-66.15° N<sup>2</sup> (d-  
 453 f) and 61.5-61.6° N<sup>2</sup>. The width of the bands (13.6-19.7 km) was set so that the area of each band was 9000 km<sup>2</sup> and contained  
 454 about 1000 gridcells.

455

456  
457

**3.2.2 Detailed analysis of vegetation composition in “hotspots” with help of empirical data statistics of threatened species for selected “hotspots”**



458  
459  
460  
461

**Figure 6.** Satellite-based (GLCE, 2nd column) and simulated (column 3-5) vegetation composition in “hotspots” within four mountain areas (row 1-4) and two forest areas (row 5-6) (see Figure 1a for location), for 1995-2004 and for two future periods following RCP8.5. Each area is 90 × 90 km (30 × 30 gridcells). The first column shows the official vector-based map from

462 Lantmäteriet (The overview map, open data license Creative Commons, (CC0), <https://www.lantmateriet.se/en/>, accessed  
463 [2021-09-09](https://www.lantmateriet.se/en/)).

464

465 According to the GLCE satellite-based product, the shrub tundra class forms a large fraction of the vegetation  
466 next to the boreal needle-leaved forest (Figure 6, Table S7a-d). The official maps from Sweden  
467 ([https://www.lantmateriet.se/en/maps-and-geographic-information/geodataprodukter/produktlista/oversik-  
468 tskartan/](https://www.lantmateriet.se/en/maps-and-geographic-information/geodataprodukter/produktlista/oversik-<br/>468 tskartan/)) show forest for parts of this area, e.g. in the valleys of the Abisko area.

469

470 For the Vindeln and Helags hotspots, the simulated distribution of forest was close to the satellite-based reference,  
471 but for the Fulu hotspot there are just a few gridcells simulated as vegetation other than boreal forest. For  
472 Björnlandet the mixture of broad-leaved trees in the forest is of similar magnitude but with a different pattern.  
473 The extent of sedge tundra was larger in the simulations than for the GLCE reference for the three northern moun-  
474 tain sites.

475

476 By 2041-2050 a significant shrubification occurs in Abisko, Vindeln and Helags (Figure 6), and forests start to  
477 establish at the edges of the current shrub and tundra vegetation, an advancement that accelerates until the 2091-  
478 2100 period.

479

480 In Abisko the needle-leaf shrub class reached a coverage of approx. 45% of the land area at the end of the century,  
481 expanding mainly over former broadleaf shrub, tundra and bare soil classes (Table S7a). In Vindeln and Helags  
482 the evergreen needle-leaf forest reaches approx. 80% coverage of the assessed area in 2091-2100 (Table S7b-c).  
483 In the boreal forest below the Fulu mountain and in the Muddus and Björnlandet areas, we see that the needle-  
484 leaf forest becomes more mixed with broad-leaved trees (Figure 6, Table S7d-f), which is also shown by higher  
485 Shannon Diversity Index ( $D$ , Table 3). ~~It should be noted that the bog class, which is well represented has a large  
486 fraction in Muddus, is excluded from the calculation of  $D$  as it is prescribed and not dynamic. Including this class  
487 would increase  $D$  but we would not be able to correctly assess the change over time. prescribed from data with  
488 0.125° resolution (see material and methods) and is therefore constant in our simulations.~~

489

490 For the northernmost hotspot studied, Abisko, the bare soil and rock class will almost disappear in the RCP8.5  
491 scenario, but most other classes will remain in similar proportions of the gridcells, though with a shift within the  
492 hotspot area (Table S7a). This is reflected in a minor increase in  $D$  (Table 3) from 1.69 to 1.75 for this hotspot.  
493 Vindeln and Helags will see a clear decrease in diversity as needle leaved forest and shrubs will come to dominate  
494 (Table 3). For Fulu and the forests hotspots an increase in diversity is projected as the forests will be more mixed.

495

496 **Table 3.** The Shannon Diversity Index ( $D$ ) calculated from the fractional cover of GLCE vegetation classes (see S7) of the  
497 “hotspots”. ~~Classes with non-dynamical vegetation like water and bogs were not included in the calculation.~~

	Abisko	Vindeln	Helags	Fulu	Muddus	Björnlandet
Satellite-based class 2000	1.44	1.38	1.42	0.50	0.14	0.80
LPJ-GUESS simulation 1995-2004	1.69	1.72	1.25	0.32	0.50	1.19

LPJ-GUESS simulation 2091-2100      1.75      0.66      0.52      0.83      0.65      1.29

498

499 Vindeln was the area with the lowest number of reported species, whereas Helags was the most diverse area with  
500 over 70% more species reported than for Vindeln (Table 4). The four other sites all had fairly equal numbers of  
501 reported species, in the range of 5155-5647 species. However, all hotspots had a similar share of red listed species  
502 and threatened species, approximately 8-10% and 3-4%, respectively (Table 4).

503

504 Of all threatened species in Sweden (2764 species), only 5.2% (144 species) are classified as alpine and almost  
505 2/3 of these threatened alpine species were found in Abisko, comprising more than half of all the threatened  
506 species in Abisko. For Vindeln and Helags, the number of threatened alpine species was just below 20%, whereas  
507 the southernmost mountain hotspot Fulu, together with the forest hotspots Muddus and Björnlandet, had less than  
508 10% of their threatened species classified as alpine.

509

510 With respect to the species groups to which most of the threatened species belong, it can be noted that mosses  
511 contribute the largest number of species in Abisko (Table 4). Except Vindeln, where birds consist of the group  
512 with most threatened species, fungi represent the largest number of threatened species for the other four hotspot  
513 areas. ~~It should be kept in mind that the data obtained from the Analysis Portal relies on what has been reported  
514 by a large community of public and professional naturalists, which means that biases can exist e.g., depending on  
515 the specific biological interests of rapporteurs visiting the different areas.~~

516

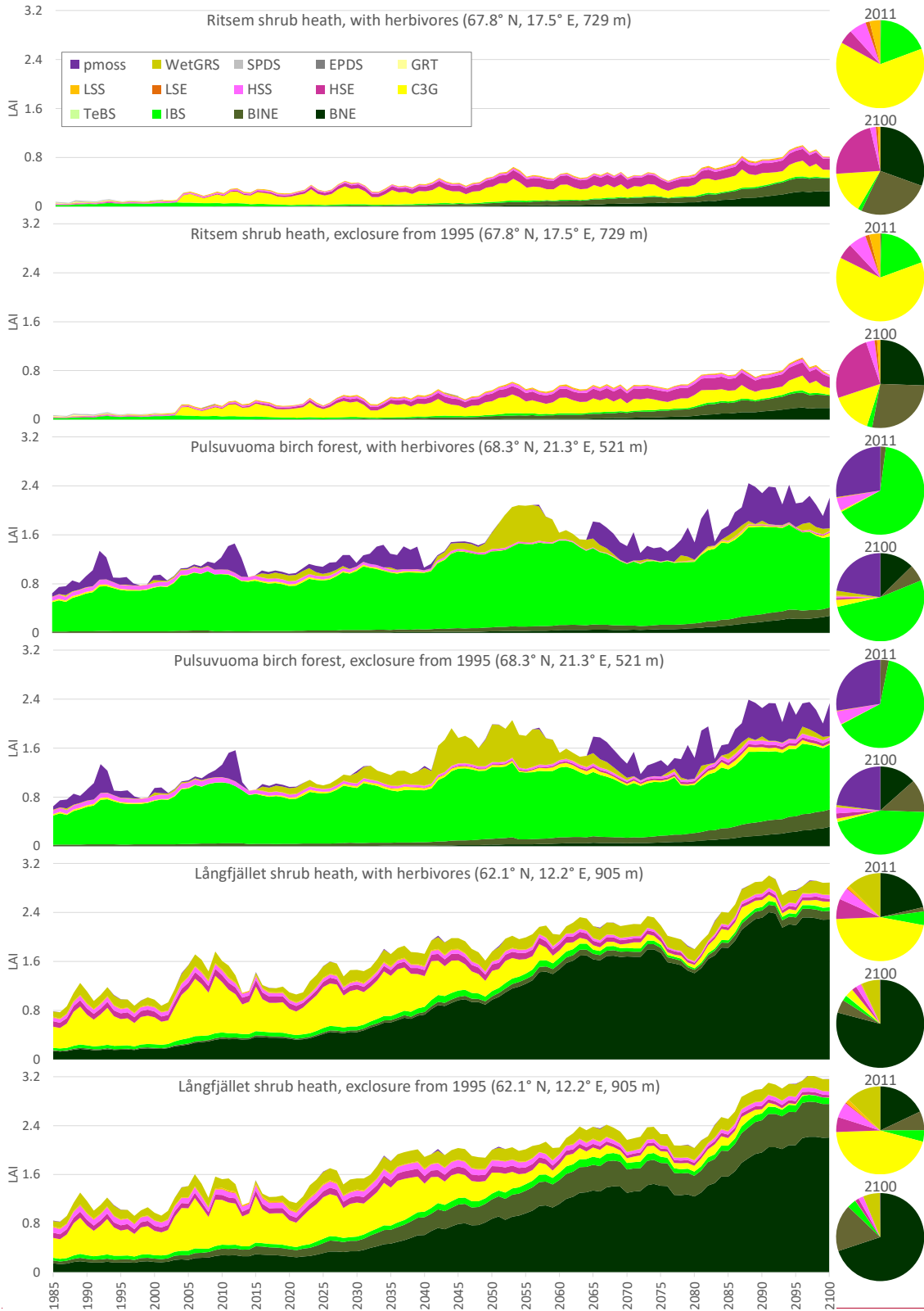
517 **Table 4.** Threatened species (VU=vulnerable, EN=endangered, CR=critically endangered) reported across species groups as  
518 well as total number of species and red-listed species reported for the six biodiversity hotspot areas.

Species group	Abisko			Vindeln			Helags			Fulu			Muddus			Björnlandet		
	VU	EN	CR	VU	EN	CR	VU	EN	CR	VU	EN	CR	VU	EN	CR	VU	EN	CR
Birds	20	11	3	24	14	3	28	13	3	23	14	3	25	14	4	20	10	2
Fungi	12	2		27	2	1	57	7	1	52	9	4	63	10	2	39	5	
Insects	19	5		22	1		21	6		19	3		37	10		23	11	
Lichens	8	2	1	16	4		29	16	7	24	10	1	14	5		14	4	
Mosses	40	9	1	6	1		33	9		16	6	1	5	3	1	5	2	
Vascular plants	18	7		10	4		17	11	1	26	12	3	8	5		8	1	1
Other groups	1			1	1		2	1		1	1		3	1		2	1	1
Threatened species (% of total)	159	3.1%		137	3.4%		262	3.7%		229	4.4%		210	3.7%		149	2.8%	
of which are alpine species	91	57%		25	18%		51	19%		20	9%		19	9%		9	6%	
Red listed species (% of total)	423	8.2%		369	9.1%		651	9.3%		528	10%		547	9.7%		411	7.8%	
Total reported species	5155			4058			7034			5205			5647			5250		

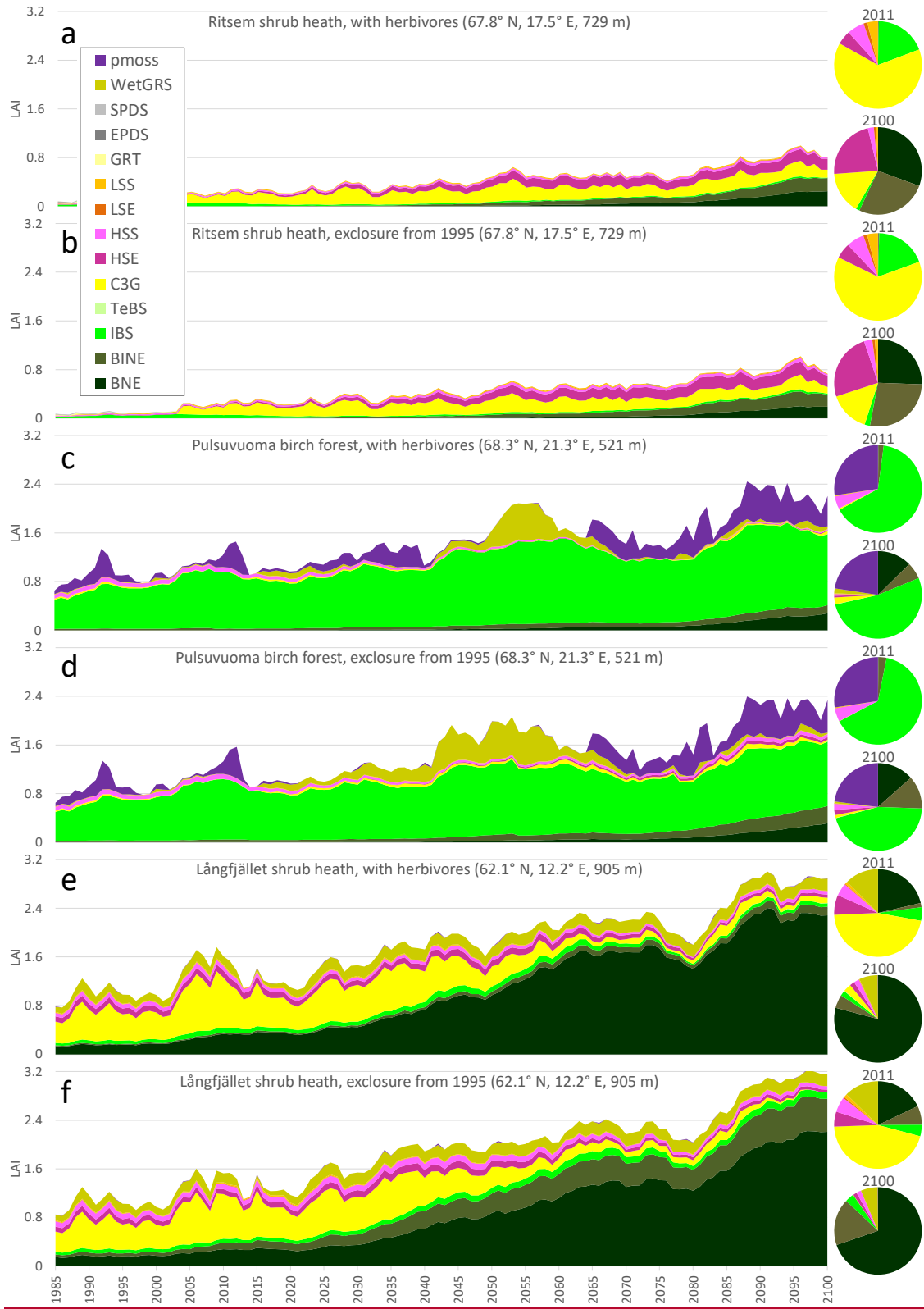
519

520 **3.3 Simulations of reindeer presence**

521



522



523

524

525

526

**Figure 7.** Simulated development of the vegetation composition (based on LAI for different PFTs, see Table 2 for description) at selected gridcells in the enclosure experiments 1985-2100, for RCP8.5.



527 **3.3.1 Simulated Effect on vegetation at reindeer enclosure sites 1985-2100**

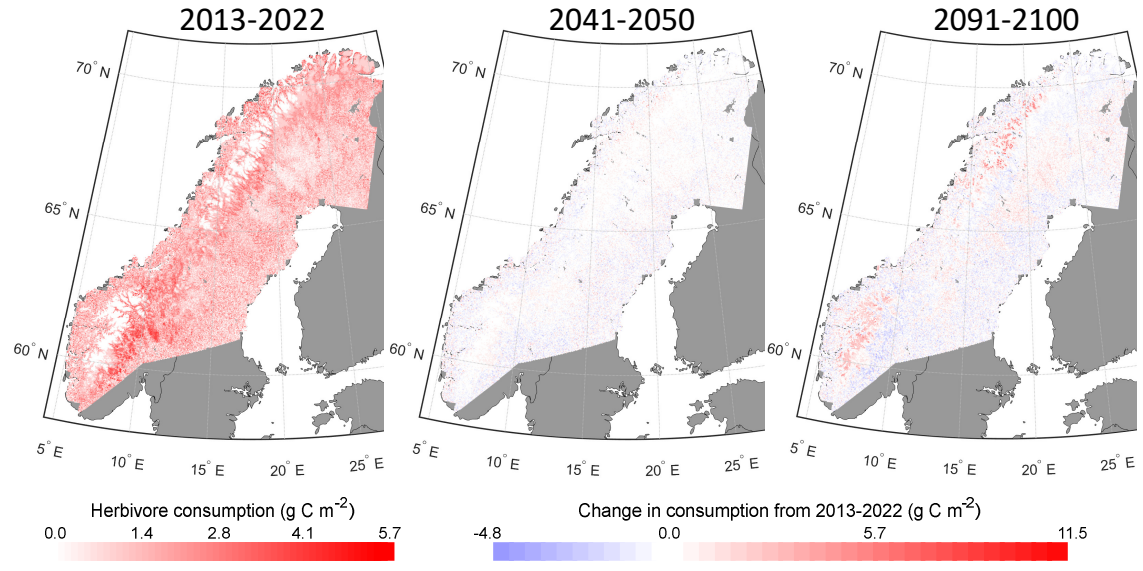
528 Three gridcells within the enclosure experiments with a wide range of conditions were selected to exemplify the  
529 simulated development of the vegetation composition until 2100 (Figure 7). Simulated LAI for the Ritsem shrub  
530 heath indicates a steep increase in year 2003, corresponding to an establishment of C3 grass, after which this PFT  
531 has a rather constant LAI over the simulation period (Figure 7a-b). Shrub vegetation (PFTs LSS, LSE (both low  
532 shrubs), HSS and HSE (tall shrubs)) increases gradually at Ritsem, ~~and, a.~~ At all sites, deciduous shrubs would  
533 have a higher fraction without simulated reindeer grazing and trampling but the difference is minor.

534  
535 The mountain birch PFT (IBS) dominates simulations for the Pulsuvuoma birch forest over the simulation period  
536 (Figure 7c-d), but for the heath gridcells there is no period with a high fraction of mountain birch forests (Figure  
537 7a-b, e-f). Instead PFTs that represent the needle-leaved coniferous forest (BNE and BINE) start to establish at  
538 the Ritsem and Pulsuvuoma gridcells around 2035 and these PFTs are already present in the simulations for  
539 Långfjället, and at the end of the simulation they are dominant at both shrub heath sites. The summer-green prostrate  
540 dwarf shrub PFT (SPDS) has a maximum fraction of ca 50% of LAI at Ritsem, though with a very sparse  
541 coverage, before C3 grass takes over, but apart from that, short shrubs (LSS and LSE), prostrate dwarf shrubs  
542 (SPDS and EPDS) and the graminoid and forb tundra (GRT) PFTs have only a minor presence in the simulations.

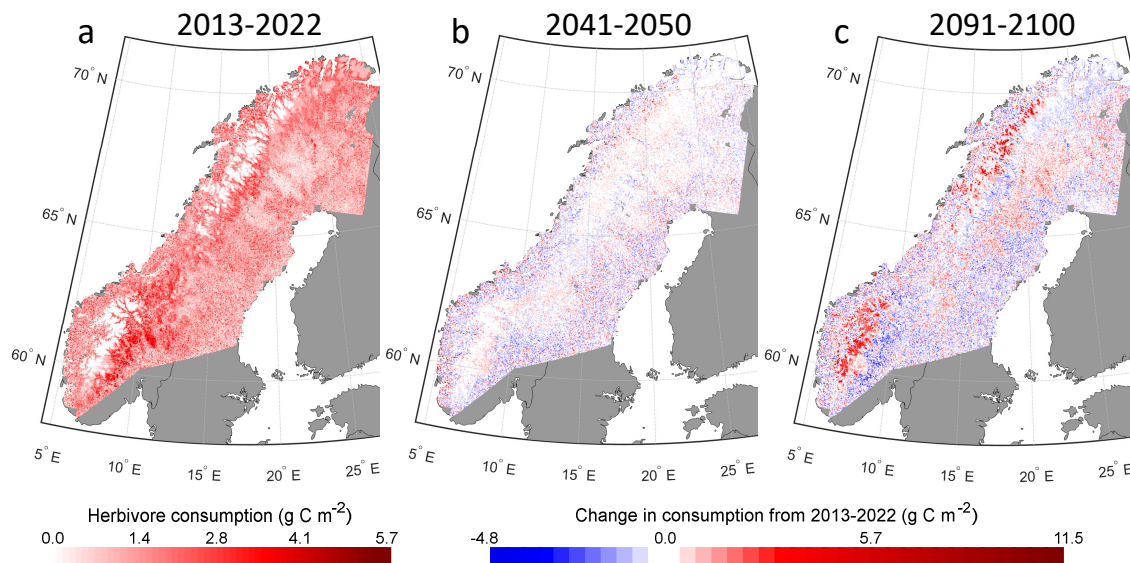
544 **3.3.2 Trends in simulated potential reindeer leaf consumption grazing 2000-2100**

545 With a constant grazing pressure, simulated reindeer leaf consumption of a PFT depends on available leaf mass,  
546 accessibility of the leaves (height less than 2.5 m) and how appetizing it is (preference value – see Table S3). In  
547 the current climate the highest consumption was found east of the mountain range with an increasing gradient  
548 from north to south (Figure 8a).

549



550



551

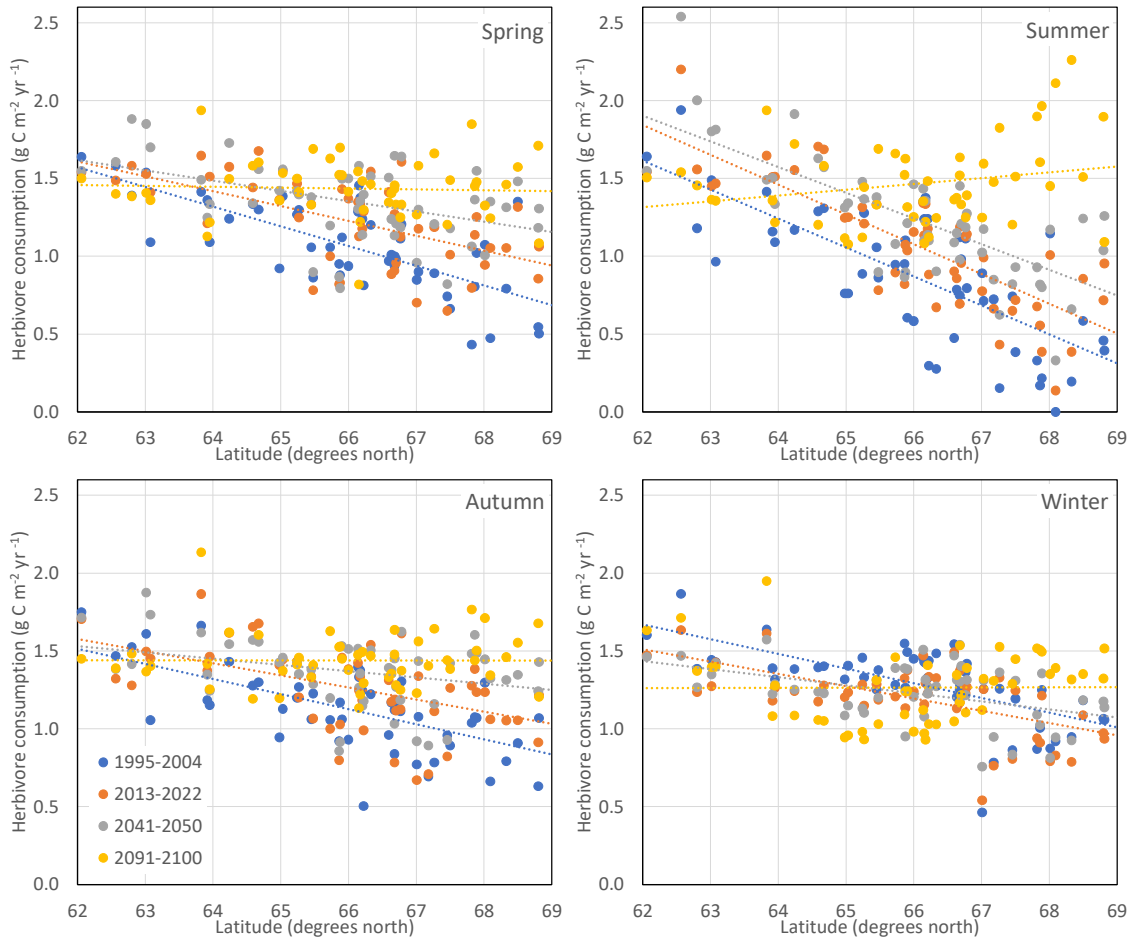
552 **Figure 8.** Simulated potential reindeer consumption ( $\text{g C m}^{-2} \text{ yr}^{-1}$ ) 2013-2022 (a) and the change to 2041-2050 (b) and 2091-  
 553 2100 (c) in RCP8.5.

554 In the boreal forest zone, the grazing level is quite evenly distributed, though there is a tendency for lower values  
 555 in areas with a higher fraction of needle-leaf PFTs (Figure 4). The change by the 2041-2050 period is small,  
 556 though some increased potential in the least vegetated areas can be seen (Figure 8b). By the end of the century  
 557 there is a substantial increase in potential consumption in the higher altitude areas as well as in the inland boreal  
 558 forest (Figure 8c). In the south and towards the east there is a trend towards reduced potential reindeer consump-  
 559 tion in the forested cells.

560

561 The traditional spring and autumn grazing grounds of the Swedish reindeer-herding communities overlap to a  
 562 high degree (Figure 1b) and both have a latitudinal dependency in potential reindeer consumption that is gradually  
 563 reduced and eventually disappears by the end of the century (Figure 9a, c). For the summer grazing grounds there  
 564 is a clear latitudinal dependency that is shifted in parallel (i.e. potential consumption increases uniformly) until  
 565 the 2041-2050 period, but by the end of the century the latitudinal trend is gone or becomes negative, with higher  
 566 potential consumption in the northern part of the study region (Figure 9b). For the winter grazing grounds, the  
 567 latitudinal dependencies are weak and the southern communities have a trend of reduced potential grazing over  
 568 time (Figure 9d). A more detailed compilation of the changes for the individual communities is given in S8.

569



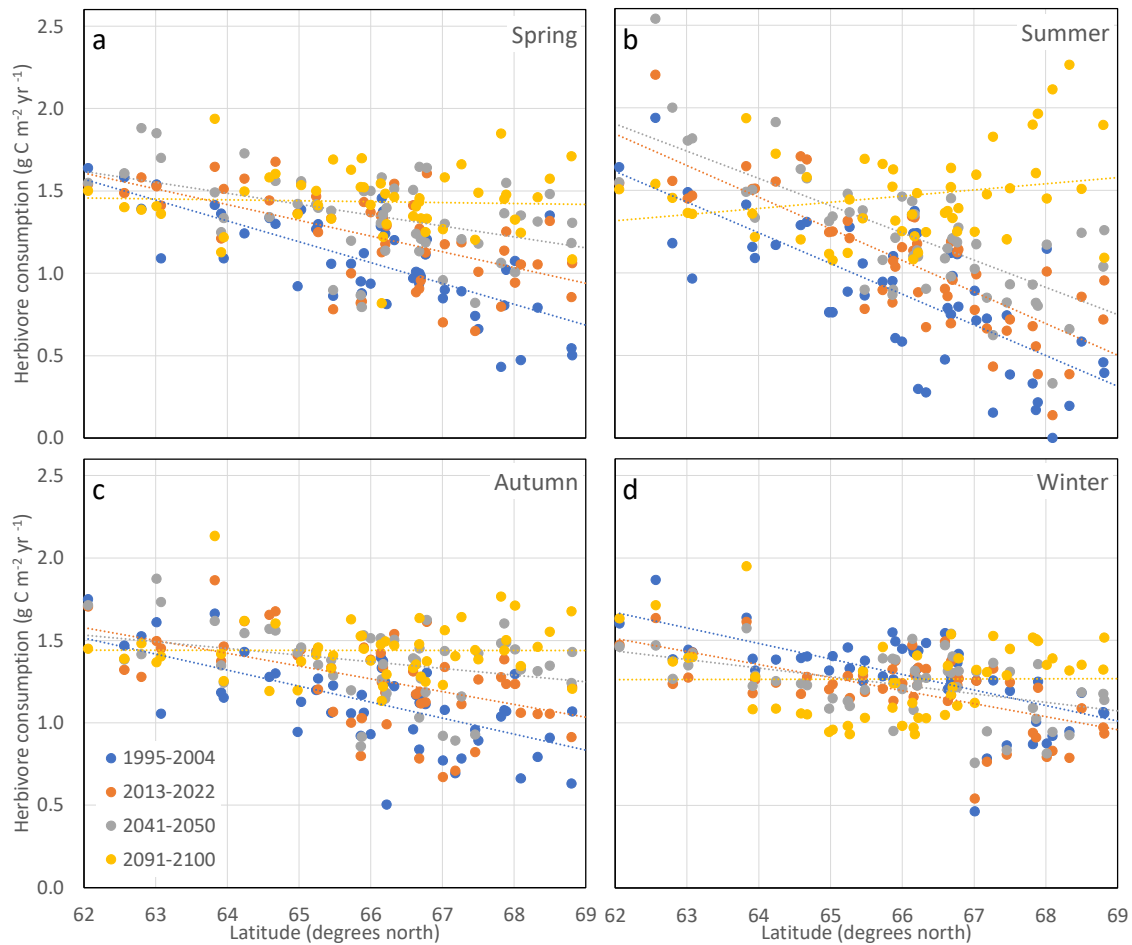


**Figure 9.** Simulated average potential reindeer consumption of leaf biomass in the 51 reindeer-herding communities in Sweden for the different seasonal grazing grounds (sub-picture a-d) and four time periods (colour) in RCP8.5.

#### 4 Discussion

The simulated changes in vegetation composition at the end of the century are dramatic-extensive in our high-emission RCP8.5 scenario. For instance, we see a successive change in forest composition, from a cover of almost purely evergreen trees to a cover containing a larger fraction of broadleaved and mixed forest by the end of the century at the alpine Fulu and low elevation Muddus and Björnlandet hotspots. In Sweden, conifers are highly favoured by forestry for traditional and economic reasons, though pine forest regenerations are already encountering large problems (e.g. from moose grazing and diseases), which can further contribute to an increase of broadleaved forests in the future (Ara et al., 2022). Our results show that a profound vegetation change will occur at the southern alpine hotspots Vindeln, Helags, and Fulu, with the most dramatic changes projected for Helags and Vindeln. Here, a rapid tree growth and expansion is observed in this scenario, with only a few tundra-denoted grids remaining by 2091-2100. This change is also associated with a strong reduction in landscape diversity, as indicated by a decrease in the vegetation-class based Shannon diversity index. Today, the largest continuous

588 Fennoscandian Low Arctic tundra areas are found between the Swedish high mountains and the border between  
589 Finland and Sweden at latitudes around 68.5 °N and in the northern and western parts of the Finnmarksvidda  
590 plateau in the north of Norway. In a changed climate, the edges of the tundra area have probably become "Scan-  
591 dinavianized" (Vuorinen et al., 2017), i.e. the coverage of dwarf birches and lichens has decreased, while the  
592 *Ericaceae* species have increased. ~~The thawing palsas in the area (Luoto and Seppälä, 2003; Oivimo et al., 2020)~~  
593 ~~are also melting faster in area. This is an ecosystem that is extremely vulnerable to the impact of warming, and at~~  
594 ~~high risk of being irreversibly lost.~~ In the simulations, the tundra remaining in Helags and Vindeln will be domi-  
595 nated by needle-leaf evergreen shrubs with just a few scattered sedge tundra areas (e.g., wet tundra areas). These  
596 results are similar to the results from long-term warming experiments and monitoring plots in the northern Scan-  
597 des, where most communities showed a "heathification" with time, both in the experimental warming and under  
598 ambient conditions subjected to the ongoing temperature increase (Scharn et al., 2021). At Fulu, the relatively  
599 extensive alpine tundra areas are situated just above the tree-line today, and here the tundra will be completely  
600 lost following RCP8.5. Thus, with a continued warming of up to 5 K to the end of the century in our model  
601 domain, which is not totally unlikely as the world is currently on track for a 2.9 K global warming (United-  
602 Nations-Environment-Programme, 2023) and given the Arctic warming amplification (Rantanen et al., 2022), the  
603 Fennoscandian vegetation is likely to far from current trend/trajectory, the Fennoscandian vegetation will undergo  
604 a rapid shifts.

605

606 The simulated change in the extent of vegetation zones is driven by establishment of PFTs, but the richness of  
607 newly established vegetation depends on the migration of all associated types of organisms. The distance species  
608 need to spread to keep up with the shifts in climate is much shorter in mountainous than in flat regions, and since  
609 the ability to spread and inhabit new regions varies among species, a loss in species richness only occurs if new  
610 immigrants are stronger competitors than the intrinsic species (Pauli and Halloy, 2019). Though total reported  
611 species richness is largest in the Helags biodiversity hotspot area and lowest in Vindeln, both have equal fractions  
612 of alpine species. Although being the best available database, it should be kept in mind that the data obtained  
613 from the Analysis Portal relies on what has been reported by a large community of public and professional natu-  
614 ralists, which means that biases can exist e.g., depending on the specific biological interests of rapporteurs visiting  
615 the different areas. As they share the same trajectories, it seems likely that the homogenization of the vegetation  
616 composition in the Helags and Vindeln areas will lead to profound shifts in the conditions for many species,  
617 especially for the alpine species occurring here. In contrast to the southern alpine hotspots, our modelling results  
618 indicate that the northernmost hotspot area Abisko likely will retain large areas of alpine vegetation at higher  
619 elevations and its landscape diversity could even slightly increase. A substantial transformation of the vegetation  
620 cover is however also expected for Abisko. This includes shrubification, a process that has already been observed  
621 in this region (Hedenås et al., 2011; Rundqvist et al., 2011; Scharn et al., 2022; Scharn et al., 2021), and the  
622 broadleaved forest moving up well above 1000 m a.s.l. from the current level of about 600-800 m (Callaghan et  
623 al., 2013), a treeline advance that also been noted in regional high resolution simulations of Abisko (Gustafson et  
624 al., 2021). Abisko is the hotspot with the largest fraction of threatened alpine species in our study, and given the  
625 large elevation span in the region there are possibilities that some species may survive in microrefugia (Mee and  
626 Moore, 2014). Our results imply that a revision of the red-list and threatened species categories is urgent. This is

627 because many of the alpine species in the hotspots areas that are not listed today will be threatened as warming  
628 continues (Schwager and Berg, 2019).

629  
630 The simulated potential reindeer consumption shows a striking increase in the summer grazing ground north of  
631 ca 65.5 °N. Although the simulated potential reindeer consumption is high, it is in the range of what can be  
632 estimated from the current reindeer population in Sweden. Today, reindeer husbandry is practiced in about 50%  
633 of the Swedish land area (i.e. 225 000 km<sup>2</sup>, [www.sametinget.se/rennaring\\_sverige](http://www.sametinget.se/rennaring_sverige)) and the population is 225 000  
634 – 280 000 animals in winter ([www.sametinget.se/rennaring\\_sverige](http://www.sametinget.se/rennaring_sverige)). With a consumption of 3-5 kg biomass per  
635 reindeer and day (Yu et al., 2017), this equals an average total consumption over the area of about 0.8 g C m<sup>-2</sup> yr<sup>-1</sup>,  
636 a number likely underestimated ~~since~~ as the livestock is larger in summer before autumn slaughter. However,  
637 in our simulations of potential reindeer winter consumption, the trends were weak both in latitude and time. Using  
638 a constant herbivory intensity in the simulations means that the potential reindeer consumption shown represents  
639 a hypothetical case in which we investigate how much would be consumed of the amount that is actually present  
640 if the same number of reindeers and the same amount of food of the same quality is present in all gridcells. This  
641 means that we have not considered mitigation and adaptation factors that may be of great importance such as  
642 climate feedbacks on the population size and changes in what land areas the reindeer feed (Bråthen et al., 2017;  
643 [Reindeer grazing, browsing and trampling may also cause indirect feedback to the climate by affecting the vegetation and ground properties, which in turn affects snow cover, albedo, carbon cycling and biogenic volatile organic compound emissions](#) (Brachmann et al., 2023; Holmgren et al., 2023)).  
644 The representation of available reindeer food in the forested winter grazing grounds is challenging. In our simulations, the potential reindeer consumption mainly consists of grasses that occur for a period after the random disturbances (with an average 150-year interval), but grasses are not the preferred reindeer food during winter. Instead, reindeer eat lichens in winter, which naturally can form dense layers under forests in the region. Current forest management, creating a dense and uniform tree cover, disturbs the growth of lichens (Kumpula et al., 2014). Furthermore, our weak trends during winter also depend on a delicate balance between a general increased productivity and higher density of the tree canopies. This balance is also important for the implementation of ground lichen PFTs, since there is a negative relationship between forest density and lichen abundance (Sandström et al., 2016). Thus, future improvements to simulations considering reindeer grazing would need: a better representation of winter forage by developing a new lichen PFT (e.g. Porada et al., 2016); an improved light-interception scheme; forest management functionality and scenarios (e.g. Lindeskog et al., 2021); and a representation of restricted access to the field and bottom layer vegetation during periods of difficult snow conditions. Though the simulated potential reindeer consumption does not show dramatic shifts over the simulated period, reindeer herding will nevertheless experience climate and weather related challenges in the future with e.g. concerns for hot and dry summers, more frequent freeze-thaw cycles and rain-on snow events during winters, as well as expanding and denser forests (Käyhkö and Horstkotte, 2017; Rosqvist et al., 2021). Thus, to be able to tackle and understand future challenges for reindeer herding this not only suggests a need to include trophic interactions in models, but it also suggests that it is crucial to evaluate the impact of extreme events on other important aspects of the environment for reindeer herding than vegetation state alone.

666 We show the benefit of using high-resolution climate data to drive our DVM, enabling the simulation of a diverse  
667 landscape, exemplified by our hotspot analysis (which would have less than 4 gridcells at a typical RCM resolution  
668 of 50x50 km). Climate representation has also improved. In particular, the simulated precipitation patterns in  
669 coastal and mountain areas as well as the ratio between snow and rainfall at high altitude show significantly better  
670 agreement with observations at higher resolutions (Lind et al., 2020). Thus, highly resolved climate data in com-  
671 bination with a state-of-the-art dynamical vegetation model clearly contributes to a better understanding of cli-  
672 mate-vegetation interactions in mountainous regions. ~~There is, however, uncertainty at many levels in this type of  
673 study: What emission scenario will the future follow and is it adequately interpreted by the global and regional  
674 climate models? Is the vegetation's direct response to climate, CO<sub>2</sub> concentration, and nitrogen deposition ade-  
675 quately described in the DVM? How will secondary effects of climate change alter disturbance patterns and land  
676 use? Due to computational limitations in this high-resolution application, it has not been possible to quantify these  
677 uncertainties (e.g. we only have one climate scenario), but it is clear from earlier studies and our results that all  
678 these aspects are important. The direction in which the results point is, however, clear in most aspects.~~

679  
680 Using the detailed classification from GLCE, the accuracy scores for the simulated vegetation classes compared  
681 to the satellite product are low. For such a large area and high resolution as in the present study, an evaluation  
682 against satellite products is the only alternative with a complete coverage, but the satellite classes cannot be con-  
683 sidered a real “ground truth”. An example of possible misclassification of the GLCE data is clear from the fact  
684 that the mountain-birch forest in some of the valleys is classified as shrub vegetation, most clearly seen for Abisko  
685 and Vindeln when compared to the official vector-based maps. The shrub and tundra ecosystems have many  
686 subclasses and the model has some difficulty in reproducing the satellite-based pattern for these. Furthermore, the  
687 parameterization of the PFTs representing these systems is based on global or regional implementations driven  
688 by monthly climate data at coarse spatial scale (Wolf et al., 2008; Zhang et al., 2013), and it is not surprising that  
689 the results call for some model adjustment. The comparisons of results from the simulations with and without  
690 reindeer presence against exclosure site data do not show conclusive results. By only remove leaf biomass, we  
691 may have underestimated the effect of browsing, which particularly effects the height development of deciduous  
692 shrubs (Vowles et al., 2017). To study the effect of reindeer exclosures *in situ* also has some experimental con-  
693 straints and uncertainty (Stark et al., 2023), e.g. as also other grazers like the hare or the lemming can have sig-  
694 nificant impact on the vegetation (Olofsson et al., 2012; Vowles et al., 2016). A further limitation of the vegetation  
695 simulations is that a soil layer always is present. The strong expansion of shrubs on former “bare soil & rock” and  
696 “permanent snow/ice” classes, e.g. as predicted for the Abisko area, is, therefore, probably overestimated, and  
697 instead parts of this area would become some type of tundra associated with shallow soils. Dispersal capacity and  
698 fire disturbance are also factors that may restrict vegetation expansion, as integration of those processes in an  
699 extrapolation of current trends in Alaska and western Canada reduced the predicted shrub expansion on non-shrub  
700 tundra from 39 to 25% by 2100 (Liu et al., 2022). In LPJ-GUESS, new PFTs can establish when climatic condi-  
701 tions are met, as we assume seeds are always present. Taking seed dispersal into account will in general slow  
702 down migration rates (Epstein et al., 2007; Zani et al., 2022). In mountainous terrain the distances will, however,  
703 be shorter and less dependent on dispersal capacity, e.g. reflected in abounded observations of tree seedlings more  
704 than 100 m above the treeline in Scandinavian mountains (Hofgaard et al., 2009). The disturbance return interval  
705 is an important and uncertain parameter that varies in time and space, which affects carbon stocks, the balance

706 between shade tolerant and intolerant species as well as plant establishment (Pugh et al., 2019). Recent studies  
707 have suggested longer intervals (Pugh et al., 2019), but there are also studies that show fire return intervals of 50-  
708 90 years in boreal forest in Sweden (Dubber et al., 2017). There are also a lot of other activities that may prevent  
709 the establishment of new plants like soil processes, seed predation, plant browsing and mortality by smaller ani-  
710 mals like rodents and hares, pests, pathogens, snow damage, moose, et cetera, which could be of potential im-  
711 portance. There is also a positive bias in the nitrogen deposition scenario (Andersson et al., 2023, manuscript) that  
712 could have further enhanced the simulated rate at which higher vegetation types expand (Gustafson et al., 2021).  
713 In the boreal forest region, the simulations have a higher fraction of broadleaf trees than the reference. A reason  
714 for this is that more than 90% of these forests are managed and needle-leaved trees are favoured in planting and  
715 thinning (Hannerz and Ekström, 2021) whereas the simulations represent natural, unmanaged vegetation where  
716 broadleaf trees are common during the regeneration phase after disturbances in boreal forest (Angelstam and  
717 Kuuluvainen, 2004). However, notwithstanding these limitations, our simulations clearly show that for Fen-  
718 noscandia, the RCP8.5 pathway results in more prominent temperate features in the boreal forest, and that these  
719 will expand northwards and to higher altitude resulting in a significant loss in tundra.

## 721 **5 Conclusions**

722 Our application of highly resolved climate data greatly improved both the representation of climate conditions  
723 and the variation in simulated vegetation in mountainous landscapes. Climate and environmental change con-  
724 sistent with the high-emission RCP8.5 scenario could cause dramatic shifts in the vegetation composition of the  
725 Fennoscandian boreal and mountain regions, with consequences for reindeer herding, forestry and tourism sec-  
726 torsour society, and implications for recreation, how we should practise conservation, and how we should manage  
727 our northern ecosystems. Indeed, these changes have already started and been observed, but they will accelerate  
728 during the 21<sup>st</sup> century. Following a climate trajectory in line with RCP8.5, the southern and lower elevation parts  
729 of the Fennoscandian mountain range that today have tundra vegetation will be covered by forests in the coming  
730 century, while high-elevation regions will undergo intense shrubification. In the northern tundra regions, most  
731 vegetation types will still be present at the end of the century but shift in altitude and be compressed to smaller  
732 regions. This will threaten already vulnerable species, especially those with slow dispersal rates and low compet-  
733 itive ability. In the southern part of the study area a massive loss of alpine habitats and species is expected. The  
734 question is rather what new vegetation types and species could occupy this area under continued climate change.  
735 There is, however, uncertainty at many levels in this type of study: What emission scenario will the future follow-  
736 hold and is it adequately interpreted by the global and regional climate models? Is the vegetation's direct response  
737 to climate, CO<sub>2</sub> concentration, and nitrogen deposition adequately described in the DVM? How will secondary  
738 effects of climate change alter disturbance patterns and land use? Due to computational limitations in this high-  
739 resolution application, it has not been possible to quantify these uncertainties (e.g. we only have one climate  
740 scenario), but it is clear from our results and those from previous earlier studies and our results that all these aspects  
741 are important. The direction in which the results point is, however, clear in most aspects. The rate of actual vege-  
742 tation changes will also depend on factors such as forest management, reindeer husbandry, other disturbances  
743 (such as fire) and the dispersal rate of different species. Our results indicate trends towards increasing amounts of



744 suitable reindeer forage, at least in northern Sweden, but other changes resulting from climate change, such as the  
745 extent of open landscapes, heat stress and altered snow conditions are likely to impact reindeer herding practises  
746 more than forage availability. The expected and potentially additive pressures of environmental changes call for  
747 scenario-based research where the main drivers of the development, including climate change, air pollution, land  
748 use and ecological processes, are considered in a consistent framework.  
749

#### 750 **Code availability**

751 The LPJ-GUESS code used and developed in this study is archived in the LPJ-GUESS Community Repository  
752 on Zenodo: <https://zenodo.org/record/8262590> (Lagergren et al., 2023). More information about the model can  
753 be found at <https://web.nateko.lu.se/lpj-guess> (LPJ-GUESS developers, 2021).  
754

#### 755 **Data availability**

756 A selection of the MATCH-BIODIV dataset and the MATCH-ECLAIRE (Engardt et al., 2017) datasets are ar-  
757 chived in Zenodo (MATCH-BIODIV: <https://zenodo.org/record/7573171> and MATCH-ECLAIRE: [https://ze-  
759 nodo.org/record/4501636#.ZBqvOXbMJaQ](https://ze-<br/>758 nodo.org/record/4501636#.ZBqvOXbMJaQ)). The ALADIN and AROME H-CLIM climate datasets (Lind et al.,  
760 2022), and the complete MATCH-BIODIV nitrogen deposition dataset (Andersson et al., 2023, manuscript) were  
761 generously shared with the authors but are not publicly accessible; the data can be accessed upon inquiry to the  
762 authors. The ECLIPSE V6b nitrogen deposition data are available from IIASA ([https://previ-  
764 ous.iiasa.ac.at/web/home/research/researchPrograms/air/ECLIPSEv6b.html](https://previ-<br/>763 ous.iiasa.ac.at/web/home/research/researchPrograms/air/ECLIPSEv6b.html)) and the NGCD data used for bias  
765 correction of temperature can be accessed at the MET Norway Thredds Service  
766 (<https://thredds.met.no/thredds/catalog/ngcd/catalog.html>). The FAO soil texture data are available at the  
767 SURFEX site (<https://www.umr-cnrm.fr/surfex/spip.php?article135>). The Corine land-cover data ([https://land.co-  
769 pernicus.eu/pan-european/corine-land-cover/clc2018](https://land.co-<br/>768 pernicus.eu/pan-european/corine-land-cover/clc2018)) and the GLCE product for northern Eurasia  
770 (<https://forobs.jrc.ec.europa.eu/products/glc2000/products.php>) are freely available. The GIS data of reindeer  
771 herding communities were obtained after personal contact with Peter Benson from the Swedish Sami Parliament  
772 ([www.sametinget.se](http://www.sametinget.se)) but are not freely available. Vegetation cover data (Vowles et al., 2017) can be accessed  
773 through Environment Climate Data Sweden (<https://doi.org/10.5879/ECDS/2017-01-29.1/0>). The biomass data  
774 from the enclosure sites are not available to the public but can be accessed by personal contact with the authors  
775 (R. Björk). Species observations for the hotspots are available at “The Analysis portal for biodiversity data” da-  
776 tabase (<https://www.analysisportal.se/>). Model simulation results with LPJ-GUESS for this manuscript are stored  
777 on DataGURU: <https://dataguru.lu.se/app#BioDiv-S> (Lagergren and Miller, 2023).

#### 776 **Author contribution**

777 FL and PAM designed the study with contribution from RGB, CA, MPB, EK, HP and GR. FL carried out the  
778 vegetation model development, setup, runs and data analysis with support from PAM. RGB extracted and analysed

779 the biodiversity data with help from MPB and HP. DB, PL and DL provided the climate scenario and associated  
780 soil and vegetation attributes. CA and TO provided high-resolution nitrogen deposition data. FL carried out bias  
781 correction and filling of continuous climate and nitrogen deposition data with advice from DB, EK and CA. RGB,  
782 MPB and GR contributed with expertise in reindeer husbandry and its interaction with the vegetation. FL prepared  
783 the manuscript with input from all co-authors.

784

#### 785 **Short summary**

786 The Fennoscandian boreal and mountain regions harbour a wide range of ecosystems sensitive to climate change.  
787 A new, highly resolved high-emission climate scenario enabled modelling of the vegetation development in this  
788 region at high resolution for the 21st century. The results show dramatic south to north and low to high altitude  
789 shifts of vegetation zones, especially for the open tundra environments, that will have large implications for nature  
790 conservation, reindeer husbandry and forestry.

791

#### 792 **Acknowledgement**

793 This work was supported by the BioDiv-Support project funded through the 2017-2018 Belmont Forum and Bi-  
794 odivERsA joint call for research proposals, under the BiodivScen ERA-Net COFUND programme, and with the  
795 funding organisations AKA (contract no 326328), ANR (ANR-18-EBI4-0007), BMBF (KFZ: 01LC1810A),  
796 FORMAS (contract no:s 2018-02434, 2018-02436, 2018-02437, 2018-02438) and MICINN (through APCIN:  
797 PCI2018-093149). The work is a contribution to the strategic research areas MERGE and BECC, and the profile  
798 area Nature-based Future Solutions hosted by Lund University. We thank Peter Benson at Sametinget for provid-  
799 ing data of the reindeer husbandry districts in Sweden and Mora Aronsson, Debora Arlt, and Johan Nilsson for  
800 advice regarding the extraction of data from the “The Analysis portal for biodiversity data”.

801

#### 802 **References**

803 Andersson, C., Langner, J., and Bergström, R.: Interannual variation and trends in air pollution over Europe due  
804 to climate variability during 1958-2001 simulated with a regional CTM coupled to the ERA40 reanalysis, *Tellus*  
805 *Series B-Chemical and Physical Meteorology*, 59, 77-98, <https://doi.org/10.1111/j.1600-0889.2006.00231.x>,  
806 2007.

807 Andersson, C., Bergström, R., Bennet, C., Robertson, L., Thomas, M., Korhonen, H., Lehtinen, K. E. J., and  
808 Kokkola, H.: MATCH-SALSA - Multi-scale Atmospheric Transport and CHemistry model coupled to the SALSA  
809 aerosol microphysics model - Part 1: Model description and evaluation, *Geoscientific Model Development*, 8,  
810 171-189, <https://doi.org/10.5194/gmd-8-171-2015>, 2015.

811 Andersson, C., Olenius, T., Alpfjord Wylde, H., Almroth Rosell, E., Björk, R. G., Björkman, M. P., Moldan, F.,  
812 and Engardt, M.: Long-term nitrogen deposition to northern Europe with focus on the Baltic Sea and the  
813 Scandinavian Mountains: reanalysis for the years 1983-2013 and comparison to multi-century (1900-2051) model  
814 simulations, Manuscript.

815 Angelstam, P. and Kuuluvainen, T.: Boreal forest disturbance regimes, successional dynamics and landscape  
816 structures - a European perspective, *Ecological Bulletins*, 51, 117-136, <https://doi.org/10.2307/20113303>, 2004.

817 Ara, M., Barbeito, I., Kalén, C., and Nilsson, U.: Regeneration failure of Scots pine changes the species  
818 composition of young forests, *Scandinavian Journal of Forest Research*, 37, 14-22,  
819 <https://doi.org/10.1080/02827581.2021.2005133>, 2022.

820 Bartalev, S. A., Belward, A. S., Erchov, D. V., and Isaev, A. S.: A new SPOT4-VEGETATION derived land  
821 cover map of Northern Eurasia, *International Journal of Remote Sensing*, 24, 1977-1982,  
822 <https://doi.org/10.1080/0143116031000066297>, 2003.

823 Barthelemy, H., Stark, S., Michelsen, A., and Olofsson, J.: Urine is an important nitrogen source for plants  
824 irrespective of vegetation composition in an Arctic tundra: Insights from a N-15-enriched urea tracer experiment,  
825 *Journal of Ecology*, 106, 367-378, <https://doi.org/10.1111/1365-2745.12820>, 2018.

826 Belušić, D., de Vries, H., Dobler, A., Landgren, O., Lind, P., Lindstedt, D., Pedersen, R. A., Sánchez-Perrino, J.  
827 C., Toivonen, E., van Ulft, B., Wang, F. X., Andrae, U., Batrak, Y., Kjellström, E., Lenderink, G., Nikulin, G.,  
828 Pietikäinen, J. P., Rodríguez-Camino, E., Samuelsson, P., van Meijgaard, E., and Wu, M. C.: HCLIM38: a flexible  
829 regional climate model applicable for different climate zones from coarse to convection-permitting scales,  
830 *Geoscientific Model Development*, 13, 1311-1333, <https://doi.org/10.5194/gmd-13-1311-2020>, 2020.

831 Bjorkman, A. D., García, C. M., Myers-Smith, I. H., Ravolainen, V., Svala Jónsdóttir, I., Westergaard, K. B.,  
832 Lawler, J. P., Aronsson, M., Bennett, B., Gardfjell, H., Heiðmarsson, S., Stewart, L., and Normand, S.: Status and  
833 trends in Arctic vegetation: Evidence from experimental warming and long-term monitoring, *Ambio*, 49, 678-  
834 692, <https://doi.org/10.1007/s13280-019-01161-6>, 2020.

835 Bjorkman, A. D., Myers-Smith, I. H., Elmendorf, S. C., Normand, S., Rueger, N., Beck, P. S. A., Blach-  
836 Overgaard, A., Blok, D., Cornelissen, J. H. C., Forbes, B. C., Georges, D., Goetz, S. J., Guay, K. C., Henry, G. H.  
837 R., HilleRisLambers, J., Hollister, R. D., Karger, D. N., Kattge, J., Manning, P., Prevey, J. S., Rixen, C.,  
838 Schaeppman-Strub, G., Thomas, H. J. D., Vellend, M., Wilmsking, M., Wipf, S., Carbognani, M., Hermanutz, L.,  
839 Levesque, E., Molau, U., Petraglia, A., Soudzilovskaia, N. A., Spasojevic, M. J., Tomaselli, M., Vowles, T.,  
840 Alatalo, J. M., Alexander, H. D., Anadon-Rosell, A., Angers-Blondin, S., te Beest, M., Berner, L., Bjork, R. G.,  
841 Buchwal, A., Buras, A., Christie, K., Cooper, E. J., Dullinger, S., Elberling, B., Eskelinen, A., Frei, E. R., Grau,  
842 O., Grogan, P., Hallinger, M., Harper, K. A., Heijmans, M. M. P. D., Hudson, J., Huelber, K., Iturrate-Garcia, M.,  
843 Iversen, C. M., Jaroszynska, F., Johnstone, J. F., Jorgensen, R. H., Kaarlejarvi, E., Klady, R., Kuleza, S., Kulonen,  
844 A., Lamarque, L. J., Lantz, T., Little, C. J., Speed, J. D. M., Michelsen, A., Milbau, A., Nabe-Nielsen, J., Nielsen,  
845 S. S., Ninot, J. M., Oberbauer, S. F., Olofsson, J., Onipchenko, V. G., Rumpf, S. B., Semenchuk, P., Shetti, R.,

846 Collier, L. S., Street, L. E., Suding, K. N., Tape, K. D., Trant, A., Treier, U. A., Tremblay, J.-P., Tremblay, M.,  
847 Venn, S., Weijers, S., Zamin, T., Boulanger-Lapointe, N., Gould, W. A., Hik, D. S., Hofgaard, A., Jonsdottir, I.  
848 S., Jorgenson, J., Klein, J., Magnusson, B., Tweedie, C., Wookey, P. A., Bahn, M., Blonder, B., van Bodegom, P.  
849 M., Bond-Lamberty, B., Campetella, G., Cerabolini, B. E. L., Chapin, F. S., III, Cornwell, W. K., Craine, J.,  
850 Dainese, M., de Vries, F. T., Diaz, S., Enquist, B. J., Green, W., Milla, R., Niinemets, U., Onoda, Y., Ordóñez, J.  
851 C., Ozinga, W. A., Penuelas, J., Poorter, H., Poschlod, P., Reich, P. B., Sande, B., Schamp, B., Sheremetev, S.,  
852 and Weiher, E.: Plant functional trait change across a warming tundra biome, *Nature*, 562, 57-62,  
853 <https://doi.org/10.1038/s41586-018-0563-7>, 2018.

854 Brachmann, C. G., Vowles, T., Rinnan, R., Björkman, M. P., Ekberg, A., and Björk, R. G.: Herbivore-shrub  
855 interactions influence ecosystem respiration and biogenic volatile organic compound composition in the subarctic,  
856 *Biogeosciences*, 20, 4069-4086, <https://doi.org/10.5194/bg-20-4069-2023>, 2023.

857 Bråthen, K. A., Ravolainen, V. T., Stien, A., Tveraa, T., and Ims, R. A.: Rangifer management controls a climate-  
858 sensitive tundra state transition, *Ecological Applications*, 27, 2416-2427, <https://doi.org/10.1002/eap.1618>, 2017.

859 Callaghan, T. V., Gatti, R. C., and Phoenix, G.: The need to understand the stability of arctic vegetation during  
860 rapid climate change: An assessment of imbalance in the literature, *Ambio*, 51, 1034-1044,  
861 <https://doi.org/10.1007/s13280-021-01607-w>, 2022.

862 Callaghan, T. V., Jonasson, C., Thierfelder, T., Yang, Z., Hedenås, H., Johansson, M., Molau, U., Van Bogaert,  
863 R., Michelsen, A., Olofsson, J., Gwynn-Jones, D., Bokhorst, S., Phoenix, G., Bjerke, J. W., Tømmervik, H.,  
864 Christensen, T. R., Hanna, E., Koller, E. K., and Sloan, V. L.: Ecosystem change and stability over multiple  
865 decades in the Swedish subarctic: complex processes and multiple drivers, *Philosophical Transactions of the*  
866 *Royal Society B-Biological Sciences*, 368, 20120488, <https://doi.org/10.1098/rstb.2012.0488>, 2013.

867 Congalton, R. G.: A review of assessing the accuracy of classifications of remotely sensed data, *Remote Sensing*  
868 *of Environment*, 37, 35-46, [https://doi.org/10.1016/0034-4257\(91\)90048-b](https://doi.org/10.1016/0034-4257(91)90048-b), 1991.

869 Constable, A. J., Harper, S., Dawson, J., Holsman, K., Mustonen, T., Piepenburg, D., and Rost, B.: Cross-Chapter  
870 Paper 6: Polar Regions, in: *Climate Change 2022: Impacts, Adaptation and Vulnerability. Contribution of*  
871 *Working Group II to the Sixth Assessment Report of the Intergovernmental Panel on Climate Change*, edited by:  
872 Pörtner, H.-O., Roberts, D. C., Tignor, M., Poloczanska, E. S., Mintenbeck, K., Alegría, A., Craig, M., Langsdorf,  
873 S., Löschke, S., Möller, V., Okem, A., and Rama, B., Cambridge University Press., Cambridge, UK and New  
874 York, NY, USA., 2319-2368, <https://doi.org/10.1017/9781009325844.023>, 2022.

875 Denryter, K. A., Cook, R. C., Cook, J. G., and Parker, K. L.: Straight from the caribou's (*Rangifer tarandus*)  
876 mouth: detailed observations of tame caribou reveal new insights into summer-autumn diets, *Canadian Journal of*  
877 *Zoology*, 95, 81-94, <https://doi.org/10.1139/cjz-2016-0114>, 2017.

878 Dobrowski, S. Z., Littlefield, C. E., Lyons, D. S., Hollenberg, C., Carroll, C., Parks, S. A., Abatzoglou, J. T.,  
879 Hegewisch, K., and Gage, J.: Protected-area targets could be undermined by climate change-driven shifts in

880 ecoregions and biomes, *Communications Earth & Environment*, 2, <https://doi.org/10.1038/s43247-021-00270-z>,  
881 2021.

882 Dubber, W., Eklundh, L., and Lagergren, F.: Comparing field inventory with mechanistic modelling and light-use  
883 efficiency modelling based approaches for estimating forest net primary productivity at a regional level, *Boreal*  
884 *Environment Research* 22, 337-352, 2017.

885 Egelkraut, D., Barthelemy, H., and Olofsson, J.: Reindeer trampling promotes vegetation changes in tundra  
886 heathlands: Results from a simulation experiment, *Journal of Vegetation Science*, 31, 476-486,  
887 <https://doi.org/10.1111/jvs.12871>, 2020.

888 Eichler, A., Legrand, M., Jenk, T. M., Preunkert, S., Andersson, C., Eckhardt, S., Engardt, M., Plach, A., and  
889 Schwikowski, M.: Consistent histories of anthropogenic western European air pollution preserved in different  
890 Alpine ice cores, *The Cryosphere*, 17, 2119-2137, <https://doi.org/10.5194/tc-17-2119-2023>, 2023.

891 Elmendorf, S. C., Henry, G. H. R., Hollister, R. D., Björk, R. G., Boulanger-Lapointe, N., Cooper, E. J.,  
892 Cornelissen, J. H. C., Day, T. A., Dorrepaal, E., Elumeeva, T. G., Gill, M., Gould, W. A., Harte, J., Hik, D. S.,  
893 Hofgaard, A., Johnson, D. R., Johnstone, J. F., Jonsdottir, I. S., Jorgenson, J. C., Klanderud, K., Klein, J. A., Koh,  
894 S., Kudo, G., Lara, M., Levesque, E., Magnusson, B., May, J. L., Mercado-Diaz, J. A., Michelsen, A., Molau, U.,  
895 Myers-Smith, I. H., Oberbauer, S. F., Onipchenko, V. G., Rixen, C., Schmidt, N. M., Shaver, G. R., Spasojevic,  
896 M. J., Porhallsdottir, P. E., Tolvanen, A., Troxler, T., Tweedie, C. E., Villareal, S., Wahren, C.-H., Walker, X.,  
897 Webber, P. J., Welker, J. M., and Wipf, S.: Plot-scale evidence of tundra vegetation change and links to recent  
898 summer warming, *Nature Climate Change*, 2, 453-457, <https://doi.org/10.1038/nclimate1465>, 2012.

899 Engardt, M., Simpson, D., Schwikowski, M., and Granat, L.: Deposition of sulphur and nitrogen in Europe 1900-  
900 2050. Model calculations and comparison to historical observations, *Tellus Series B-Chemical and Physical*  
901 *Meteorology*, 69, 1328945, <https://doi.org/10.1080/16000889.2017.1328945>, 2017.

902 Epstein, H. E., Yu, Q., Kaplan, J. O., and Lischke, H.: Simulating future changes in Arctic and subarctic  
903 vegetation, *Computing in Science & Engineering*, 9, 12-23, <https://doi.org/10.1109/mcse.2007.84>, 2007.

904 Eriksson, O., Niva, M., and Caruso, A.: Use and abuse of reindeer range, *Acta Phytogeographica Suecica*, 87, 1-  
905 110, 2007.

906 Faroux, S., Kaptué Tchuenté, A. T., Roujean, J.-L., Masson, V., Martin, E., and Le Moigne, P.: ECOCLIMAP-  
907 II/Europe: a twofold database of ecosystems and surface parameters at 1 km resolution based on satellite  
908 information for use in land surface, meteorological and climate models, *Geoscientific Model Development*, 6,  
909 563-582, <https://doi.org/10.5194/gmd-6-563-2013>, 2013.

910 Feeley, K. J., Silman, M. R., Bush, M. B., Farfan, W., Cabrera, K. G., Malhi, Y., Meir, P., Revilla, N. S.,  
911 Quisiyupanqui, M. N. R., and Saatchi, S.: Upslope migration of Andean trees, *Journal of Biogeography*, 38, 783-  
912 791, <https://doi.org/10.1111/j.1365-2699.2010.02444.x>, 2011.

913 Ferraro, K. M., Schmitz, O. J., and McCary, M. A.: Effects of ungulate density and sociality on landscape  
914 heterogeneity: a mechanistic modeling approach, *Ecography*, 2022, e06039, <https://doi.org/10.1111/ecog.06039>,  
915 2022.

916 Flower-Ellis, J. G. K. and Olsson, L.: Estimation of volume, total and projected area of Scots pine needles from  
917 their regression on length, *Studia Forestalia Suecica*, 190, 1-19, 1993.

918 Fohringer, C., Rosqvist, G., Inga, N., and Singh, N. J.: Reindeer husbandry in peril?-How extractive industries  
919 exert multiple pressures on an Arctic pastoral ecosystem, *People and Nature*, 3, 872-886,  
920 <https://doi.org/10.1002/pan3.10234>, 2021.

921 George, J.-P., Yang, W., Kobayashi, H., Biermann, T., Carrara, A., Cremonese, E., Cuntz, M., Fares, S., Gerosa,  
922 G., Grünwald, T., Hase, N., Heliasz, M., Ibrom, A., Knohl, A., Kruijt, B., Lange, H., Limousin, J.-M., Loustau,  
923 D., Lukeš, P., Marzuoli, R., Mölder, M., Montagnani, L., Neiryneck, J., Peichl, M., Rebmann, C., Schmidt, M.,  
924 Serrano, F. R. L., Soudani, K., Vincke, C., and Pisek, J.: Method comparison of indirect assessments of understory  
925 leaf area index (LAI(u)): A case study across the extended network of ICOS forest ecosystem sites in Europe,  
926 *Ecological Indicators*, 128, <https://doi.org/10.1016/j.ecolind.2021.107841>, 2021.

927 Gustafson, A., Miller, P. A., Björk, R., Olin, S., and Smith, B.: Nitrogen restricts future sub-arctic treeline advance  
928 in an individual-based dynamic vegetation model, *Biogeosciences*, 18, 6329–6347, <https://doi.org/10.5194/bg-18-6329-2021>, 2021.

930 Hannerz, M. and Ekström, H.: Nordic Forest Statistics 2020 – Resources, Industry, Trade, Conservation, and  
931 Climate, *Nordic Forest Research*, 32, 2021.

932 Hazeleger, W., Wang, X., Severijns, C., Ștefănescu, S., Bintanja, R., Sterl, A., Wyser, K., Semmler, T., Yang, S.,  
933 van den Hurk, B., van Noije, T., van der Linden, E., and van der Wiel, K.: EC-Earth V2.2: description and  
934 validation of a new seamless earth system prediction model, *Climate Dynamics*, 39, 2611-2629,  
935 <https://doi.org/10.1007/s00382-011-1228-5>, 2012.

936 Hazeleger, W., Severijns, C., Semmler, T., Ștefănescu, S., Yang, S., Wang, X., Wyser, K., Dutra, E., Baldasano,  
937 J. M., Bintanja, R., Bougeault, P., Caballero, R., Ekman, A. M. L., Christensen, J. H., van den Hurk, B., Jimenez,  
938 P., Jones, C., Källberg, P., Koenigk, T., McGrath, R., Miranda, P., Van Noije, T., Palmer, T., Parodi, J. A.,  
939 Schmith, T., Selten, F., Storelvmo, T., Sterl, A., Tapamo, H., Vancoppenolle, M., Viterbo, P., and Willén, U.: EC-  
940 Earth A Seamless Earth-System Prediction Approach in Action, *Bulletin of the American Meteorological Society*,  
941 91, 1357-1363, <https://doi.org/10.1175/2010bams2877.1>, 2010.

942 Hedenås, H., Olsson, H., Jonasson, C., Bergstedt, J., Dahlberg, U., and Callaghan, T. V.: Changes in Tree Growth,  
943 Biomass and Vegetation Over a 13-Year Period in the Swedish Sub-Arctic, *Ambio*, 40, 672-682,  
944 <https://doi.org/10.1007/s13280-011-0173-1>, 2011.

945 Hickler, T., Vohland, K., Feehan, J., Miller, P. A., Smith, B., Costa, L., Giesecke, T., Fronzek, S., Carter, T. R.,  
946 Cramer, W., Kühn, I., and Sykes, M. T.: Projecting the future distribution of European potential natural vegetation

947 zones with a generalized, tree species-based dynamic vegetation model, *Global Ecology and Biogeography*, 21,  
948 50-63, <https://doi.org/10.1111/j.1466-8238.2010.00613.x>, 2012.

949 Hofgaard, A., Dalen, L., and Hytteborn, H.: Tree recruitment above the treeline and potential for climate-driven  
950 treeline change, *Journal of Vegetation Science*, 20, 1133-1144, <https://doi.org/10.1111/j.1654-1103.2009.01114.x>, 2009.

952 Höglund-Isaksson, L., Gómez-Sanabria, A., Klimont, Z., Rafaj, P., and Schöpp, W.: Technical potentials and  
953 costs for reducing global anthropogenic methane emissions in the 2050 timeframe -results from the GAINS model,  
954 *Environmental Research Communications*, 2, 025004, <https://doi.org/10.1088/2515-7620/ab7457>, 2020.

955 Holmgren, M., Groten, F., Carracedo, M. R., Vink, S., and Limpens, J.: Rewilding Risks for Peatland Permafrost,  
956 *Ecosystems*, <https://doi.org/10.1007/s10021-023-00865-x>, 2023.

957 Hudson, J. M. G. and Henry, G. H. R.: Increased plant biomass in a High Arctic heath community from 1981 to  
958 2008, *Ecology*, 90, 2657-2663, <https://doi.org/10.1890/09-0102.1>, 2009.

959 Huttunen, L., Ayres, M. P., Niemelä, P., Heiska, S., Tegelberg, R., Rousi, M., and Kellomäki, S.: Interactive  
960 effects of defoliation and climate change on compensatory growth of silver birch seedlings, *Silva Fennica*, 47,  
961 <https://doi.org/10.14214/sf.964>, 2013.

962 IPCC: Annex II: Climate System Scenario Tables, in: *Climate Change 2013: The Physical Science Basis. Contribution of Working Group I to the Fifth Assessment Report of the Intergovernmental Panel on Climate Change*, edited by: Prather, M., Flato, G., Friedlingstein, P., Jones, C., Lamarque, J.-F., Liao, H., and Rasch, P., Cambridge University Press, Cambridge, United Kingdom and New York, NY, USA, 2013.

966 IPCC: *Climate Change 2014: Synthesis Report. Contribution of Working Groups I, II and III to the Fifth Assessment Report of the Intergovernmental Panel on Climate Change* [Core Writing Team, R.K. Pachauri and L.A. Meyer (eds.)]. Geneve, 151 pp.2014.

969 Johansson, T.: Biomass production and allometric above- and below-ground relations for young birch stands  
970 planted at four spacings on abandoned farmland, *Forestry*, 80, 41-52, <https://doi.org/10.1093/forestry/cpl049>,  
971 2007.

972 Käyhkö, J. and Horstkotte, T.: Reindeer husbandry under global change in the tundra region of Northern  
973 Fennoscandia, *Publications from the Department of Geography and Geology, University of Turku.*, 40,  
974 <https://doi.org/https://doi.org/10.13140/RG.2.2.22151.39841>, 2017.

975 Kosztra, B., Büttner, G., Hazeu, G., and Arnold, S.: Updated CLC illustrated nomenclature guidelines, European  
976 Topic Centre on Urban, land and soil systems, 126, 2019.

977 Kullman, L.: Ecological overview of past and recent history of the alpine tree line ecotone and plant cover in the  
978 Swedish Scandes (In Swedish with English summary), *Svensk Botanisk Tidsskrift*, 110, 132-272, 2016.

979 Kumpula, J., Kurkilahti, M., Helle, T., and Colpaert, A.: Both reindeer management and several other land use  
980 factors explain the reduction in ground lichens (*Cladonia* spp.) in pastures grazed by semi-domesticated reindeer  
981 in Finland, *Regional Environmental Change*, 14, 541-559, <https://doi.org/10.1007/s10113-013-0508-5>, 2014.

982 Kuuluvainen, T. and Gauthier, S.: Young and old forest in the boreal: critical stages of ecosystem dynamics and  
983 management under global change, *Forest Ecosystems*, 5, 26, <https://doi.org/10.1186/s40663-018-0142-2>, 2018.

984 Lagergren, F. and Miller, P. A.: LPJ-GUESS model results with arctic plant functional types (PFTs) for  
985 Fennoscandia from the BioDiv-Support project at RCP 8.5, DataGURU, <https://doi.org/10.18161/j395-1j66>,  
986 2023.

987 Lagergren, F., Olin, S., and Miller, P. A.: Incorporating reindeer grazing and damage by ozone in LPJ-GUESS  
988 for the BioDiv-Support project, Zenodo, <https://doi.org/10.5281/zenodo.8262590>, 2023.

989 Lamarque, J. F., Kyle, G. P., Meinshausen, M., Riahi, K., Smith, S. J., van Vuuren, D. P., Conley, A. J., and Vitt,  
990 F.: Global and regional evolution of short-lived radiatively-active gases and aerosols in the Representative  
991 Concentration Pathways, *Climatic Change*, 109, 191-212, <https://doi.org/10.1007/s10584-011-0155-0>, 2011.

992 Lamarque, J. F., Bond, T. C., Eyring, V., Granier, C., Heil, A., Klimont, Z., Lee, D., Liousse, C., Mieville, A.,  
993 Owen, B., Schultz, M. G., Shindell, D., Smith, S. J., Stehfest, E., Van Aardenne, J., Cooper, O. R., Kainuma, M.,  
994 Mahowald, N., McConnell, J. R., Naik, V., Riahi, K., and van Vuuren, D. P.: Historical (1850-2000) gridded  
995 anthropogenic and biomass burning emissions of reactive gases and aerosols: methodology and application,  
996 *Atmospheric Chemistry and Physics*, 10, 7017-7039, <https://doi.org/10.5194/acp-10-7017-2010>, 2010.

997 Lind, P., Belušić, D., Christensen, O. B., Dobler, A., Kjellström, E., Landgren, O., Lindstedt, D., Matte, D.,  
998 Pedersen, R. A., Toivonen, E., and Wang, F. X.: Benefits and added value of convection-permitting climate  
999 modeling over Fenno-Scandinavia, *Climate Dynamics*, 55, 1893-1912, <https://doi.org/10.1007/s00382-020-05359-3>,  
1000 2020.

1001 Lind, P., Pedersen, R. A., Kjellström, E., Landgren, O., Matte, D., Dobler, A., Belušić, D., Médus, E., Wang, F.,  
1002 Christensen, O. B., Christensen, J. H., and Verpe Dyrdal, A.: Climate change information over Fenno-Scandinavia  
1003 produced with a convection-permitting climate model, *Climate Dynamics*, In press,  
1004 <https://doi.org/10.1007/s00382-022-06589-3>, 2022.

1005 Lindeskog, M., Smith, B., Lagergren, F., Sycheva, E., Ficko, A., Pretzsch, H., and Rammig, A.: Accounting for  
1006 forest management in the estimation of forest carbon balance using the dynamic vegetation model LPJ-GUESS  
1007 (v4.0, r9710): implementation and evaluation of simulations for Europe, *Geoscientific Model Development*, 14,  
1008 6071-6112, <https://doi.org/10.5194/gmd-14-6071-2021>, 2021.

1009 Liu, Y., Riley, W. J., Keenan, T. F., Mekonnen, Z. A., Holm, J. A., Zhu, Q., and Torn, M. S.: Dispersal and fire  
1010 limit Arctic shrub expansion, *Nature Communications*, 13, 3843, <https://doi.org/10.1038/s41467-022-31597-6>,  
1011 2022.



- 1012 Luoto, M. and Seppälä, M.: Thermokarst ponds as indicators of the former distribution of palsas in Finnish  
1013 lapland, *Permafrost and Periglacial Processes*, 14, 19-27, <https://doi.org/10.1002/ppp.441>, 2003.
- 1014 Masson, V., Le Moigne, P., Martin, E., Faroux, S., Alias, A., Alkama, R., Belamari, S., Barbu, A., Boone, A.,  
1015 Bouyssel, F., Brousseau, P., Brun, E., Calvet, J.-C., Carrer, D., Decharme, B., Delire, C., Donier, S., Essaouini,  
1016 K., Gibelin, A.-L., Giordani, H., Habets, F., Jidane, M., Kerdraon, G., Kourzeneva, E., Lafaysse, M., Lafont, S.,  
1017 Brossier, C. L., Lemonsu, A., Mahfouf, J.-F., Marguinaud, P., Mokhtari, M., Morin, S., Pigeon, G., Salgado, R.,  
1018 Seity, Y., Taillefer, F., Tanguy, G., Tulet, P., Vincendon, B., Vionnet, V., and Voldoire, A.: The SURFEXv7.2  
1019 land and ocean surface platform for coupled or offline simulation of earth surface variables and fluxes,  
1020 *Geoscientific Model Development*, 6, 929-960, <https://doi.org/10.5194/gmd-6-929-2013>, 2013.
- 1021 McEwan, E. H. and Whitehead, P. E.: Seasonal changes in the energy and nitrogen intake in reindeer and caribou,  
1022 *Canadian Journal of Zoology*, 48, 905-913, <https://doi.org/10.1139/z70-164>, 1970.
- 1023 Mee, J. A. and Moore, J.-S.: The ecological and evolutionary implications of microrefugia, *Journal of*  
1024 *Biogeography*, 41, 837-841, <https://doi.org/10.1111/jbi.12254>, 2014.
- 1025 Meinshausen, M., Smith, S. J., Calvin, K., Daniel, J. S., Kainuma, M. L. T., Lamarque, J. F., Matsumoto, K.,  
1026 Montzka, S. A., Raper, S. C. B., Riahi, K., Thomson, A., Velders, G. J. M., and van Vuuren, D. P. P.: The RCP  
1027 greenhouse gas concentrations and their extensions from 1765 to 2300, *Climatic Change*, 109, 213-241,  
1028 <https://doi.org/10.1007/s10584-011-0156-z>, 2011.
- 1029 Miller, P. A. and Smith, B.: Modelling Tundra Vegetation Response to Recent Arctic Warming, *Ambio*, 41, 281-  
1030 291, <https://doi.org/10.1007/s13280-012-0306-1>, 2012.
- 1031 Molinari, C., Hantson, S., and Nieradzik, L. P.: Fire Dynamics in Boreal Forests Over the 20th Century: A Data-  
1032 Model Comparison, *Frontiers in Ecology and Evolution*, 9, <https://doi.org/10.3389/fevo.2021.728958>, 2021.
- 1033 Myers-Smith, I. H., Forbes, B. C., Wilmsking, M., Hallinger, M., Lantz, T., Blok, D., Tape, K. D., Macias-Fauria,  
1034 M., Sass-Klaassen, U., Lévesque, E., Boudreau, S., Ropars, P., Hermanutz, L., Trant, A., Siegwart Collier, L.,  
1035 Weijers, S., Rozema, J., Rayback, S. A., Schmidt, N. M., Schaepman-Strub, G., Wipf, S., Rixen, C., Ménard, C.  
1036 B., Venn, S., Goetz, S., Andreu-Hayles, L., Elmendorf, S., Ravolainen, V., Welker, J., Grogan, P., Epstein, H. E.,  
1037 and Hik, D. S.: Shrub expansion in tundra ecosystems: dynamics, impacts and research priorities, *Environmental*  
1038 *Research Letters*, 6, 045509, <https://doi.org/10.1088/1748-9326/6/4/045509>, 2011.
- 1039 Nord, J., Anthoni, P., Gregor, K., Gustafson, A., Hantson, S., Lindeskog, M., Meyer, B., Miller, P., Nieradzik, L.,  
1040 Olin, S., Papastefanou, P., Smith, B., Tang, J., and Wårlind, D.: LPJ-GUESS Release v4.1.1 model code, Zenodo,  
1041 <https://doi.org/10.5281/zenodo.8065737>, 2021.
- 1042 Oksanen, L. and Virtanen, R.: Topographic, altitudinal and regional patterns in continental and suboceanic heath  
1043 vegetation of northern Fennoscandia, *Acta Botanica Fennica*, 153, 1-80, 1995.

1044 Olofsson, J., Tømmervik, H., and Callaghan, T. V.: Vole and lemming activity observed from space, *Nature*  
1045 *Climate Change*, 2, 880-883, <https://doi.org/10.1038/nclimate1537>, 2012.

1046 Olofsson, J., Kitti, H., Rautiainen, P., Stark, S., and Oksanen, L.: Effects of summer grazing by reindeer on  
1047 composition of vegetation, productivity and nitrogen cycling, *Ecography*, 24, 13-24,  
1048 <https://doi.org/10.1034/j.1600-0587.2001.240103.x>, 2001.

1049 Olofsson, J., Oksanen, L., Callaghan, T., Hulme, P. E., Oksanen, T., and Suominen, O.: Herbivores inhibit climate-  
1050 driven shrub expansion on the tundra, *Global Change Biology*, 15, 2681-2693, <https://doi.org/10.1111/j.1365-2486.2009.01935.x>, 2009.

1052 Olvmo, M., Holmer, B., Thorsson, S., Reese, H., and Lindberg, F.: Sub-arctic tundra degradation and the role of  
1053 climatic drivers in the largest coherent tundra mire complex in Sweden (Vissatvuopmi), 1955-2016, *Scientific*  
1054 *Reports*, 10, 8937, <https://doi.org/10.1038/s41598-020-65719-1>, 2020.

1055 Ono, J., Watanabe, M., Komuro, Y., Tatebe, H., and Abe, M.: Enhanced Arctic warming amplification revealed  
1056 in a low-emission scenario, *Communications Earth & Environment*, 3, 27, <https://doi.org/10.1038/s43247-022-00354-4>, 2022.

1058 Osuch, M., Lawrence, D., Meresa, H. K., Napiorkowski, J. J., and Romanowicz, R. J.: Projected changes in flood  
1059 indices in selected catchments in Poland in the 21st century, *Stochastic Environmental Research and Risk*  
1060 *Assessment*, 31, 2435-2457, <https://doi.org/10.1007/s00477-016-1296-5>, 2017.

1061 Pauli, H. and Halloy, S. R. P.: High Mountain Ecosystems Under Climate Change, in: *Oxford Research*  
1062 *Encyclopedia of Climate Science*, edited by: Pauli, H., and Halloy, S. R. P., Oxford University Press, 1-56,  
1063 <https://doi.org/10.1093/acrefore/9780190228620.013.764>, 2019.

1064 Pearson, R. G., Phillips, S. J., Lorant, M. M., Beck, P. S. A., Damoulas, T., Knight, S. J., and Goetz, S. J.: Shifts  
1065 in Arctic vegetation and associated feedbacks under climate change, *Nature Climate Change*, 3, 673-677,  
1066 <https://doi.org/10.1038/nclimate1858>, 2013.

1067 Porada, P., Ekici, A., and Beer, C.: Effects of bryophyte and lichen cover on permafrost soil temperature at large  
1068 scale, *Cryosphere*, 10, 2291-2315, <https://doi.org/10.5194/tc-10-2291-2016>, 2016.

1069 Pugh, T. A. M., Arneeth, A., Kautz, M., Poulter, B., and Smith, B.: Important role of forest disturbances in the  
1070 global biomass turnover and carbon sinks, *Nature Geoscience*, 12, 730-+, <https://doi.org/10.1038/s41561-019-0427-2>, 2019.

1072 Qi, Y. L., Wei, W., Chen, C. G., and Chen, L. D.: Plant root-shoot biomass allocation over diverse biomes: A  
1073 global synthesis, *Global Ecology and Conservation*, 18, e00606, <https://doi.org/10.1016/j.gecco.2019.e00606>,  
1074 2019.

- 1075 Rantanen, M., Karpechko, A. Y., Lipponen, A., Nordling, K., Hyvärinen, O., Ruosteenoja, K., Vihma, T., and  
1076 Laaksonen, A.: The Arctic has warmed nearly four times faster than the globe since 1979, *Communications Earth  
1077 & Environment*, 3, 168, <https://doi.org/10.1038/s43247-022-00498-3>, 2022.
- 1078 Rasmus, S., Horstkotte, T., Turunen, M., Landauer, M., Löf, A., Lehtonen, I., Rosqvist, G., and Holand, Ø.:  
1079 Reindeer husbandry and climate change - Challenges for adaptation, in: *Reindeer Husbandry and Global  
1080 Environmental Change - Pastoralism in Fennoscandia*, edited by: Horstkotte, T., Holand, Ø., Kumpula, J., and  
1081 Moen, J., Routledge, London, 99-117, <https://doi.org/10.4324/9781003118565-8>, 2022.
- 1082 Robertson, L., Langner, J., and Engardt, M.: An Eulerian limited-area atmospheric transport model, *Journal of  
1083 Applied Meteorology*, 38, 190-210, [https://doi.org/10.1175/1520-0450\(1999\)038<0190:Aelaat>2.0.Co;2](https://doi.org/10.1175/1520-0450(1999)038<0190:Aelaat>2.0.Co;2), 1999.
- 1084 Rosqvist, G. C., Inga, N., and Eriksson, P.: Impacts of climate warming on reindeer herding require new land-use  
1085 strategies, *Ambio*, 51, 1247–1262, <https://doi.org/10.1007/s13280-021-01655-2>, 2021.
- 1086 Rundqvist, S., Hedenås, H., Sandström, A., Emanuelsson, U., Eriksson, H., Jonasson, C., and Callaghan, T. V.:  
1087 Tree and Shrub Expansion Over the Past 34 Years at the Tree-Line Near Abisko, Sweden, *Ambio*, 40, 683-692,  
1088 <https://doi.org/10.1007/s13280-011-0174-0>, 2011.
- 1089 Sandström, P., Cory, N., Svensson, J., Hedenås, H., Jougda, L., and Borchert, N.: On the decline of ground lichen  
1090 forests in the Swedish boreal landscape: Implications for reindeer husbandry and sustainable forest management,  
1091 *Ambio*, 45, 415-429, <https://doi.org/10.1007/s13280-015-0759-0>, 2016.
- 1092 Scharn, R., Little, C. J., Bacon, C. D., Alatalo, J. M., Antonelli, A., Björkman, M. P., Molau, U., Nilsson, R. H.,  
1093 and Björk, R. G.: Decreased soil moisture due to warming drives phylogenetic diversity and community transitions  
1094 in the tundra, *Environmental Research Letters*, 16, 064031, <https://doi.org/10.1088/1748-9326/abfe8a>, 2021.
- 1095 Scharn, R., Brachmann, C. G., Patchett, A., Reese, H., Björkman, A. D., Alatalo, J. M., Björk, R. G., Jägerbrand,  
1096 A. K., Molau, U., and Björkman, M. P.: Vegetation responses to 26 years of warming at Latnjajaure Field Station,  
1097 northern Sweden, *Arctic Science*, 8, 858-877, <https://doi.org/10.1139/as-2020-0042>, 2022.
- 1098 Schwager, P. and Berg, C.: Global warming threatens conservation status of alpine EU habitat types in the  
1099 European Eastern Alps, *Regional Environmental Change*, 19, 2411-2421, <https://doi.org/10.1007/s10113-019-01554-z>, 2019.
- 1101 Shannon, C. E.: A mathematical theory of communication, *The Bell System Technical Journal*, 27, 379–423,  
1102 1948.
- 1103 Smith, B., Prentice, I. C., and Sykes, M. T.: Representation of vegetation dynamics in the modelling of terrestrial  
1104 ecosystems: comparing two contrasting approaches within European climate space, *Global Ecology and  
1105 Biogeography*, 10, 621-637, <https://doi.org/10.1046/j.1466-822X.2001.t01-1-00256.x>, 2001.

1106 Smith, B., Wårlind, D., Arneth, A., Hickler, T., Leadley, P., Siltberg, J., and Zaehle, S.: Implications of  
1107 incorporating N cycling and N limitations on primary production in an individual-based dynamic vegetation  
1108 model, *Biogeosciences*, 11, 2027-2054, <https://doi.org/10.5194/bg-11-2027-2014>, 2014.

1109 Speed, J. D. M., Austrheim, G., Kolstad, A. L., and Solberg, E. J.: Long-term changes in northern large-herbivore  
1110 communities reveal differential rewilding rates in space and time, *Plos One*, 14,  
1111 <https://doi.org/10.1371/journal.pone.0217166>, 2019.

1112 Stark, S., Horstkotte, T., Kumpula, J., Olofsson, J., Tømmervik, H., and Turunen, M.: The ecosystem effects of  
1113 reindeer (*Rangifer tarandus*) in northern Fennoscandia: Past, present and future, *Perspectives in Plant Ecology*  
1114 *Evolution and Systematics*, 58, <https://doi.org/10.1016/j.ppees.2022.125716>, 2023.

1115 Stoessel, M., Moen, J., and Lindborg, R.: Mapping cumulative pressures on the grazing lands of northern  
1116 Fennoscandia, *Scientific reports*, 12, 16044-16044, <https://doi.org/10.1038/s41598-022-20095-w>, 2022.

1117 Sturm, M., Racine, C., and Tape, K.: Climate change - Increasing shrub abundance in the Arctic, *Nature*, 411,  
1118 546-547, <https://doi.org/10.1038/35079180>, 2001.

1119 Sundqvist, M. K., Moen, J., Björk, R. G., Vowles, T., Kytöviita, M.-M., Parsons, M. A., and Olofsson, J.:  
1120 Experimental evidence of the long-term effects of reindeer on Arctic vegetation greenness and species richness at  
1121 a larger landscape scale, *Journal of Ecology*, 107, 2724-2736, <https://doi.org/10.1111/1365-2745.13201>, 2019.

1122 Tang, J., Miller, P. A., Persson, A., Olefeldt, D., Pilesjö, P., Heliasz, M., Jackowicz-Korczynski, M., Yang, Z.,  
1123 Smith, B., Callaghan, T. V., and Christensen, T. R.: Carbon budget estimation of a subarctic catchment using a  
1124 dynamic ecosystem model at high spatial resolution, *Biogeosciences*, 12, 2791-2808, <https://doi.org/10.5194/bg-12-2791-2015>, 2015.

1126 Thomas, S. C. and Martin, A. R.: Carbon Content of Tree Tissues: A Synthesis, *Forests*, 3, 332-352,  
1127 <https://doi.org/10.3390/f3020332>, 2012.

1128 United-Nations-Environment-Programme: Emissions Gap Report 2023: Broken Record – Temperatures hit new  
1129 highs, yet world fails to cut emissions (again), Nairobi, <https://doi.org/10.59117/20.500.11822/43922>, 2023.

1130 Venäläinen, A., Lehtonen, I., Laapas, M., Ruosteenoja, K., Tikkanen, O.-P., Viiri, H., Ikonen, V.-P., and Peltola,  
1131 H.: Climate change induces multiple risks to boreal forests and forestry in Finland: A literature review, *Global*  
1132 *Change Biology*, 26, 4178-4196, <https://doi.org/10.1111/gcb.15183>, 2020.

1133 Vowles, T., Molau, U., Lindstein, L., Molau, M., and Björk, R. G.: The impact of shrub browsing by mountain  
1134 hare and reindeer in subarctic Sweden, *Plant Ecology & Diversity*, 9, 421-428,  
1135 <https://doi.org/10.1080/17550874.2016.1264017>, 2016.

1136 Vowles, T., Gunnarsson, B., Molau, U., Hickler, T., Klemetsson, L., and Björk, R. G.: Expansion of deciduous  
1137 tall shrubs but not evergreen dwarf shrubs inhibited by reindeer in Scandes mountain range, *Journal of Ecology*,  
1138 105, 1547-1561, <https://doi.org/10.1111/1365-2745.12753>, 2017.

1139 Vuorinen, K. E. M., Oksanen, L., Oksanen, T., Pyykönen, A., Olofsson, J., and Virtanen, R.: Open tundra persist,  
1140 but arctic features decline-Vegetation changes in the warming Fennoscandian tundra, *Global Change Biology*, 23,  
1141 3794-3807, <https://doi.org/10.1111/gcb.13710>, 2017.

1142 Wania, R., Ross, I., and Prentice, I. C.: Integrating peatlands and permafrost into a dynamic global vegetation  
1143 model: 2. Evaluation and sensitivity of vegetation and carbon cycle processes, *Global Biogeochemical Cycles*,  
1144 23, GB3015, <https://doi.org/10.1029/2008gb003413>, 2009a.

1145 Wania, R., Ross, I., and Prentice, I. C.: Integrating peatlands and permafrost into a dynamic global vegetation  
1146 model: 1. Evaluation and sensitivity of physical land surface processes, *Global Biogeochemical Cycles*, 23,  
1147 GB3014, <https://doi.org/10.1029/2008gb003412>, 2009b.

1148 Wolf, A., Callaghan, T. V., and Larson, K.: Future changes in vegetation and ecosystem function of the Barents  
1149 Region, *Climatic Change*, 87, 51-73, <https://doi.org/10.1007/s10584-007-9342-4>, 2008.

1150 Xu, J., Morris, P. J., Liu, J., and Holden, J.: PEATMAP: Refining estimates of global peatland distribution based  
1151 on a meta-analysis, *Catena*, 160, 134-140, <https://doi.org/10.1016/j.catena.2017.09.010>, 2018.

1152 Yu, Q., Epstein, H., Engstrom, R., and Walker, D.: Circumpolar arctic tundra biomass and productivity dynamics  
1153 in response to projected climate change and herbivory, *Global Change Biology*, 23, 3895-3907,  
1154 <https://doi.org/10.1111/gcb.13632>, 2017.

1155 Zani, D., Lehsten, V., and Lischke, H.: Tree migration in the dynamic, global vegetation model LPJ-GM 1.1:  
1156 efficient uncertainty assessment and improved dispersal kernels of European trees, *Geoscientific Model*  
1157 *Development*, 15, 4913-4940, <https://doi.org/10.5194/gmd-15-4913-2022>, 2022.

1158 Zhang, W. X., Miller, P. A., Smith, B., Wania, R., Koenigk, T., and Döscher, R.: Tundra shrubification and tree-  
1159 line advance amplify arctic climate warming: results from an individual-based dynamic vegetation model,  
1160 *Environmental Research Letters*, 8, 034023, <https://doi.org/10.1088/1748-9326/8/3/034023>, 2013.

1161